INFORMATION TO USERS

This manuscript has been reproduced from the microfilm master. UMI films the text directly from the original or copy submitted. Thus, some thesis and dissertation copies are in typewriter face, while others may be from any type of computer printer.

The quality of this reproduction is dependent upon the quality of the copy submitted. Broken or indistinct print, colored or poor quality illustrations and photographs, print bleedthrough, substandard margins, and improper alignment can adversely affect reproduction.

In the unlikely event that the author did not send UMI a complete manuscript and there are missing pages, these will be noted. Also, if unauthorized copyright material had to be removed, a note will indicate the deletion.

Oversize materials (e.g., maps, drawings, charts) are reproduced by sectioning the original, beginning at the upper left-hand corner and continuing from left to right in equal sections with small overlaps.

Photographs included in the original manuscript have been reproduced xerographically in this copy. Higher quality 6" x 9" black and white photographic prints are available for any photographs or illustrations appearing in this copy for an additional charge. Contact UMI directly to order.

Bell & Howell Information and Learning
300 North Zeeb Road, Ann Arbor, MI 48106-1346 USA
800-521-0600

Developmental Expression and Functions of Voltage-gated Potassium Channels in Normal and Mutant Mice

by

Janice Lynn Hallows

A dissertation submitted in partial fulfillment of the requirements for the degree of

Doctor of Philosophy

University of Washington

1999

Program Authorized to Offer Degree: Pharmacology

UMI Number: 9983487

UMI Microform 9983487

Bell & Howell Information and Learning Company
300 North Zeeb Road
P.O. Box 1346
Ann Arbor, MI 48106-1346

Doctoral Dissertation

In presenting this dissertation in partial fulfillment of the requirements for the Doctoral degree at the University of Washington,

I agree that the Library shall make its copies freely available for inspection. I further agree that extensive copying of the dissertation is allowable only for scholarly purposes, consistent with "fair use" as prescribed in the U.S. Copyright Law. Requests for copying or reproduction of this dissertation may be referred to Bell and Howell Information and Learning, 300 North Zeeb Road, P.O. Box 1346, Ann Arbor, MI 48106-1346, to whom the author has granted "the right to reproduce and sell (a) copies of the manuscript in microform and/or (b) printed copies of the manuscript made from microform."

Signature Janice E. Hall

Date 11/19/1999

University of Washington
Graduate School

This is to certify that I have examined this copy of a doctoral dissertation by

Janice Lynn Hallows

and have found that it is complete and satisfactory in all respects,
and that any and all revisions required by the final
examining committee have been made.

Chair of Supervisory Committee:

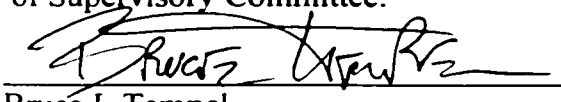

Bruce L Tempel

Reading Committee:

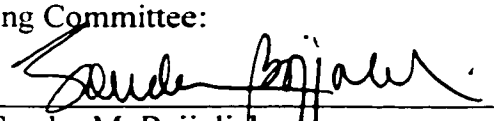

Sandra M. Bajjalieh

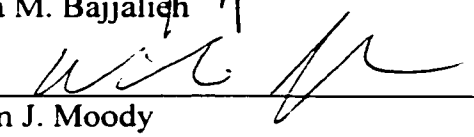

William J. Moody

Date: 11/19/1999

University of Washington

Abstract

Developmental Expression and Functions of Voltage-gated Potassium Channels in Normal and Mutant Mice

by Janice Lynn Hallows

Chairperson of the Supervisory Committee

Associate Professor Bruce L Tempel
Departments of Otolaryngology-Head and Neck Surgery and Pharmacology

Kv1.1, a Shaker-like voltage-gated potassium channel, is strongly expressed in a variety of neurons in adult rodents, where it appears to be involved in regulating neuronal excitability. Here we show that Kv1.1 is also expressed during development in the mouse, and undergoes very complex changes in expression and localization during both embryonic and postnatal development.

In the embryo, there are two transient peaks of Kv1.1 expression, occurring around embryonic day (E) 9.5 and E14.5. At E9.5, Kv1.1 RNA and protein are detected transiently in non-neuronal cells in tightly restricted segments or regions of the early central nervous system, including rhombomeres 3 and 5, the mesencephalon and the diencephalon. At E14.5, several cell types in both the central and peripheral nervous systems express Kv1.1, including neuronal cells (sensory ganglia and outer aspect of cerebral hemispheres) and glial cells (radial glia, satellite cells, Schwann cell precursors). These data show that Kv1.1 is expressed transiently in a variety of neuronal and non-neuronal cells during restricted periods of embryonic development, and the expression pattern suggests several potential developmental roles for Kv1.1. Using mice lacking

both copies of Kv1.1, we have found that this channel appears to be involved in the regulation of Schwann cell proliferation.

During postnatal development, Kv1.1 and Kv1.2 undergo a dramatic redistribution in peripheral nerves. We show here that this redistribution is a very dynamic process that involves the formation of characteristic intermediate clusters and occurs over several days time. The cues or signals responsible for the redistribution of Kv channels remain unknown. To begin to understand these signals, we have examined the distribution of both Kv1.1 and voltage-gated sodium (Na) channels in the neurological mouse mutant *quivering*. We report here that both types of ion channels are mislocalized in the sciatic nerves of mice with three different alleles of *quivering*. Second, peripheral myelin is disrupted in at least one of the *quivering* alleles. Finally, the degree of anatomical disruption in these mice correlates with the severity of the hindlimb phenotype in *quivering* mice.

TABLE OF CONTENTS

LIST OF FIGURES

Number *Page*

LIST OF TABLES

Number *Page*

LIST OF ABBREVIATIONS

^{32}P, ^{33}P	phosphorous 32 or 33
^{0}C	degrees Celsius
α	alpha
β	beta
µg	microgram
µl	microliter
µm	micrometer
ATP	adenosine triphosphate
bp	basepair
CHO	Chinese hamster ovary
CNS	central nervous system
cpm	counts per minute
Ctx	cortex
d	day(s)
D	dorsal
DNA	deoxyribonucleic acid
DRG	dorsal root ganglion
E	embryonic day
GGF	glial growth factor
H	hypothalamus
het	heterozygote
Hip	hippocampus
hr	hour
I	intermediate
ICC	immunocytochemistry
Ig	immunoglobulin
I_{Kv}	delayed rectifier or sustained outward potassium current
K^+	potassium
kHz	kilohertz
ko	knockout
Kv	voltage-gated potassium (channel)
L	large
m	meter
M	molar
mg	milligram
ml	milliliter
mm	millimeter
mM	millimolar
MNTB	medial nucleus of the trapezoid body
msec	millisecond
mV	millivolt
Na^+	sodium

ng	nanogram
P	postnatal day
PBS	phosphate buffered saline
PFA	paraformaldehyde
PI	phosphoimager
PNS	peripheral nervous system
qv	quivering
r	rhombomere
RNA	ribonucleic acid
RNase	ribonuclease
RPA	ribonuclease protection assay
S	small
SE	standard error
sec	second
TBS	tris buffered saline
TEA	tetraethylammonium
Tec	tectum
Teg	tegmentum
TEM	transmission electronmicroscopy
TG	trigeminal ganglion
Th	thalamus
V	ventral
Vnt	ventricle
wt	wildtype

ACKNOWLEDGMENTS

I wish to thank several researchers for their generous gifts of antibodies used in this work: J. H. Pate Skene (Duke University) for the anti-GAP-43 antibodies; Anthony Frankenfurter (University of Virginia) for the TuJ1 antibodies; Tom Schwarz (Stanford University) for the anti-Kv1.5 antibodies; James Trimmer (State University of New York at Stonnybrook) for antibodies to Kv1.2, Kv1.4 and Kv1.6; Rock Levinson (University of Colorado, Denver) for the anti-Na channel antibodies. The monoclonal antibodies 40E-C and RC-2 were obtained from the Developmental Studies Hybridoma Bank maintained by the Department of Pharmacology and Molecular Sciences, Johns Hopkins University School of Medicine, Baltimore, MD, and the Department of Biological Sciences, University of Iowa, Iowa City, IA, under contract N01-HD-6-2915 from the NICHD. I would also like to thank Linda Robinson, whose superb animal care made these studies possible. Many thanks go to my collaborators: Dale Cunningham (University of Washington) who performed the electronmicroscopy, and Bill Lippe (University of Washington) who helped design and perform the electrophysiological studies. Finally, I would like to thank my advisor, Bruce Tempel, for his support and guidance over the years.

CHAPTER 1: INTRODUCTION

Potassium (K^+) currents are perhaps the most diverse group of ion driven currents found in nature. They have been observed in a large number of tissues that include both excitable (neurons, muscles) and non-excitable (glia, epithelium, lymphocytes) cell types (Lewis and Cahalan, 1988; Hille, 1992; Sontheimer, 1994; Aguilar-Bryan and Bryan, 1999). A variety of current types have been identified based on kinetics and direction of current flow; currents may be sustained or transient, slowly or rapidly activating or inactivating, and current flow can be into or out of the cell. Additionally, there are several mechanisms responsible for gating of the ion channels underlying these currents, such as changes in membrane potential, ligand binding, intracellular gradients in calcium concentration, and pressure (Hille, 1992).

The huge diversity of K^+ currents coupled with the multiple mechanisms of channel gating give rise to a multitude of physiological functions for these channels. Perhaps the most widely studied functions of K^+ currents are those of voltage-gated (Kv) currents in mature neurons, where they play a role in determination of resting membrane potentials, shaping of action potentials, regulation of neuronal firing patterns, and modulation of neurotransmitter release (Hille, 1992). At least seven types of K^+-selective currents help regulate cardiac rhythm: (1) a Kv delayed rectifier current, (2) a Kv transient outward current, (3) an inward rectifier current, (4) an acetylcholine-activated inward rectifier current, (5) an ATP-sensitive current, (6) a current activated by elevated intracellular sodium levels, and (7) a calcium-activated current (Zipes, 1995). Glial cells exhibit Kv delayed rectifier, transient outward and inward rectifier currents, where they are thought to be involved in the removal and redistribution of K^+ in the brain as well as modulation of glial proliferation (Sontheimer, 1994). An ATP-sensitive K^+ current helps regulate insulin secretion from β cells in the pancreas (Aguilar-Bryan and Bryan, 1999). Activation and subsequent proliferation and differentiation of T lymphocytes is regulated by Kv and calcium-activated K^+ currents (Rader, Kahn et al., 1996).

As suggested above, Kv currents are a widely distributed subset of K^+ currents and are crucial to the functioning of muscles as well as the nervous and immune systems.

A variety of structural and physiological channel properties contribute to the diversity of Kv currents. These channels are encoded by a large family of genes whose names were originally based on their homology to the *Shaker* locus in *Drosophila*, and are divided into subfamilies named *Shaker*, *Shab*, *Shaw*, and *Shal* in flies, Kv1, Kv2, Kv3 and Kv4 in mammals, and KCNA1, KCNA2, KCNA3 and KCNA4 in humans (Chandy and Gutman, 1993). In addition to the large family of genes encoding Kv channels, there are alternatively spliced transcripts found within some subfamilies (Perney, Marshall et al., 1992; Ohya, Tanaka et al., 1997). Each of the Shaker-like Kv genes encodes a single alpha (α) peptide that consists of a hydrophobic core region of six transmembrane alpha-helices (S1-S6) bordered by cytoplasmic amino and carboxyl terminal domains. The loop between the fifth and sixth transmembrane domains is thought to dip toward the membrane and line the pore of the channel (Yellen, Jurman et al., 1991). A series of positively charged residues along the length of S4 appears to act as a voltage sensor for voltage-dependent activation (Papazian, Timpe et al., 1991). Functional channels consist of four α subunits (MacKinnon, 1991). The tetramers may be either homomultimers formed from a single type of α subunit or heteromultimers comprised of two to four distinct types of α subunits. It appears that heteromultimers can form from members of the same subfamily, but not between subfamilies (Covarrubias, Wei et al., 1991). For example, Kv1.1 can form tetramers with Kv1.2, but not with Kv2.1, Kv3.1, or Kv4.1. Each channel subunit or combination of subunits gives rise to distinct biophysical properties; there are differences in voltage dependence of activation and inactivation and kinetics (Hille, 1992). Additionally, Kv channel function may be modified by association with intracellular peptides called beta (β) subunits (Rettig, Heinemann et al., 1994).

The first mammalian Shaker-like Kv channel cloned was Kv1.1 (Baumann, Grupe et al., 1988; Tempel, Jan et al., 1988). When expressed alone in transformed mammalian cell lines or *Xenopus* oocytes, Kv1.1 forms a rapidly activating sustained outward K^+ current that is often referred to as a delayed rectifier current (Stuhmer, Stocker et al., 1988; Bosma, Allen et al., 1993; Hopkins, Allen et al., 1994). Coexpression of Kv1.1 with other members of the *Shaker* family gives rise to currents with unique properties

reflecting formation of heteromeric channels (Isacoff, Jan et al., 1990; Ruppersberg, Schroter et al., 1990). Kv1.1 can form heteromeric channels with other members of the *Shaker* family of α subunits *in vivo* (Wang, Kunkel et al., 1993; Scott, Muniz et al., 1994). Association of Kv1.1 with β subunits has been demonstrated *in vitro*, and gives rise to a rapidly inactivating current (Rettig, Heinemann et al., 1994; Heinemann, Rettig et al., 1996; Nakahira, Shi et al., 1996). Kv1.1 colocalizes with β subunits *in vivo*, suggesting a possible functional association of the two subunit types (Scott, Muniz et al., 1994; Rhodes, Monaghan et al., 1996). In mice, Kv1.1 is broadly expressed in neurons and glia of the nervous system at sites including cell somata, dendrites, synaptic terminals, unmyelinated axons, and juxtaparanodal regions of myelinated axons (Tsaur, Sheng et al., 1992; Wang, Kunkel et al., 1993; Wang, Kunkel et al., 1994; Mi, Deerinck et al., 1995; Veh, Lichtinghagen et al., 1995). The pattern of Kv1.1 distribution is unique from but overlaps with other members of the *Shaker* family of α subunits. For example, Kv1.1 and 1.2 are both localized to the dentate gyrus of the hippocampus, while in the CA3 region Kv1.1 immunoreactivity is much greater than that of Kv1.2 (Wang, Kunkel et al., 1994). Colocalization of Kv1.1 with other Shaker-like Kv subunits coupled with its broad distribution suggests this channel subunit may contribute to a large number of Kv currents identified *in vivo*.

The complexity of Kv channel structure-function relationships has made it difficult to determine which channel subunits are responsible for the currents identified *in vivo*. The unique but overlapping cellular and subcellular localizations of channel subunits has further confounded this issue. One approach to studying this question is to examine the consequences of a mutation in or deletion of a single Kv channel gene. Mutations in Kv1.1 have been identified in flies and humans, and a null mutant engineered in mice. In *Drosophila*, mutations in the *Shaker* locus result in hyperexcitability (Papazian, Schwarz et al., 1987). In humans, point mutations in the human homolog of Kv1.1, *KCNA1*, result in a disorder characterized by brief episodes of ataxia with myokymia (rippling of muscles) evident between attacks, and may predispose affected individuals to development of epilepsy (Browne, Gancher et al., 1994; Zuberi,

Eunson et al., 1999). In Kv1.1-null mice, the predominant phenotype is the occurrence of spontaneous tonic/clonic seizures; additionally, sciatic nerves from mice lacking Kv1.1 exhibit a prolonged refractory period (Smart, Lopantsev et al., 1998). These findings are consistent with the hypotheses that Kv1.1 may be involved in regulation of neuronal excitability, neurotransmitter release and axonal repolarization in adult mammals.

Similar Kv currents to those found in adults have been identified during embryonic and postnatal development (Soliven, Szuchet et al., 1989; Moody, Simoncini et al., 1991; Barish, 1995). While the expression and functions of Kv channels responsible for these currents have been extensively studied in mature animals, less is know regarding their expression patterns and functions during development. Current data indicates Kv1.1 channels are responsible for some of the Kv currents observed in non-mammalian embryos (see chapter 2 introduction); however, the expression of Kv1.1 during mammalian embryonic development has not been previously studied. Similarly, Kv1.1 may also contribute to developmental Kv currents identified in Schwann cells and peripheral nerves in mammalian neonates (Chiu, Scherer et al., 1994), and the study of the expression pattern of Kv1.1 during mammalian postnatal development has only recently begun (Vabnick, Trimmer et al., 1999). To investigate if Kv1.1 may be contributing to developmental Kv currents in mammals, we have examined expression pattern of this channel subunit during embryonic and postnatal development in mouse. Additionally, we have studied the developmental functions of this channel in mice lacking Kv1.1 and *quivering* mutants.

CHAPTER 2: EXPRESSION OF Kv1.1, A SHAKER-LIKE POTASSIUM CHANNEL, IS TEMPORALLY REGULATED IN EMBRYONIC NEURONS AND GLIA

Introduction

Several potassium (K^+) currents are developmentally regulated in non-mammalian species, including those identified in oocytes (Hagiwara, Miyasaki et al., 1975; Moody, 1985), during early cleavages (deLatt and Bluemink, 1974), around the time of gastrulation (Simoncini, Block et al., 1988), and during muscle differentiation (Ribera and Spitzer, 1991; Spruce and Moody, 1992). One of the most extensively studied K^+ currents in non-mammalian embryos is a delayed rectifier K^+ current (I_{Kv}) that is first detected during neurogenesis in amphibians. Differentiation of this current is essential for normal neuronal development; the appearance of I_{Kv} is crucial for the transition from early, long duration action potentials to mature, brief spikes (Barish, 1986; O'Dowd, Ribera et al., 1988; Lockery and Spitzer, 1992). Several lines of evidence suggest that the expression of *Xenopus* (x)Kv1.1 may play an important part in the development of I_{Kv}, and thus in neuronal development. First, developing *Xenopus* spinal neurons express xKv1.1 and xKv2.2, which are homologous in sequence and expressed currents to previously identified mammalian Kv channels, Kv1.1 and Kv2.2, respectively (Ribera and Nguyen, 1993; Burger and Ribera, 1996). The spinal neurons are homogenous with respect to development of I_{Kv} (O'Dowd, Ribera et al., 1988; Desarmenien, Clendening et al., 1993), but different Kv channels underlie I_{Kv} in different neurons. Overexpression of a dominant-negative Kv1 subunit suggests that 20% of spinal neurons express only Kv1 potassium currents (Ribera, 1996). Second, early overexpression of xKv1.1 in cultured spinal neurons results in the premature appearance of I_{Kv} and a reduction in the number of morphologically differentiated neurons (Jones and Ribera, 1994). Third, both xKv1.1 and

xKv2.2 transcripts are temporally regulated in developing spinal neurons during the period of I_{Kv} development (Gurantz, Ribera et al., 1996).

The development of I_{Kv} has been less well studied in mammals, though limited data suggest this current is essential for mammalian neuronal development as well. Delayed-rectifier currents have been identified in several types of rodent embryonic cultured neurons, including rat cortical (Zona, Eusebi et al., 1990; Rizzo and Nonner, 1992) and neostriatal neurons (Surmeier, Stefani et al., 1991), mouse hippocampal neurons (Wu and Barish, 1994), and rat and mouse spinal cord and dorsal root ganglia (DRG) neurons (Naciff, Behbehani et al., 1996); however, the molecular identity of the channel subunit types that contribute to these currents is unknown. Moreover, it is not known what other cells express delayed rectifier channels during murine development, or if their expression is temporally regulated. We show here that Kv1.1 is expressed in a complex temporal and tissue-specific pattern during murine development. Implications for possible developmental functions of Kv channels are discussed.

Materials and Methods

Animals

C_3HeB/FeJ mice obtained from Jackson Laboratories were maintained in our colony on a 12 hour light-dark cycle. Breeding pairs were established and females examined each morning for the presence of a vaginal plug. 12:00 noon on the day a plug was detected was designated embryonic day (E) 0.5, and dissections were begun around noon at indicated ages. Embryos were quickly dissected in phosphate buffered saline (PBS: 137 mM NaCl; 2.7 mM KCl; 10 mM Na_2HPO_4; 1.75 mM KH_2PO_4), homogenized in guanidinium buffer (4 M guanidinium thiocyanate; 24 mM sodium citrate, 17 mM N-lauroylsarcosine, 7% β-mercaptoethanol) for RNA isolation; quickly frozen on dry ice for *in situ* hybridization; or fixed for 2 hours in 4% paraformaldehyde in PBS for

immunocytochemistry. Whole brains from postnatal mice were quickly dissected in PBS and homogenized in guanidinium for RNA isolation.

RNA and RNase protection

The guanidinium thiocyanate method (Chomczynski and Sacchi, 1987) was used to isolate total RNA from whole brains and whole embryos at E13.5-E16.5, or pooled embryos at E8.5-E12.5. RNA concentration was determined by spectrophotometric measurement, and 0.5-1 μg of total RNA was electrophoresed on a 1% agarose/18% formaldehyde gel to verify that the RNA was intact.

A region of Kv1.1 that spans the translational start site was used as a template to generate a 310 basepair (bp) 5' antisense riboprobe that yields a 252 bp (42 bp 5' untranslated region and 210 bp open reading frame) protected fragment (Bosma, Allen et al., 1993, Wang, 1995 #16) when digested with RNases A and T1 (Ausubel, 1992). 20-25 μg of total RNA was mixed with 10^5 cpm of probe, and prior to hybridization, aliquots of samples were diluted 10^{-5} and hybridized to a 423 bp probe that protects a 350 bp fragment of 18S rRNA to monitor the amount of total RNA in samples. Gels were apposed to Hyperfilm MP (Amersham) for 4-5 days at -80 ^{0}C to generate autoradiographs, then subjected to PhosphorImager (Molecular Dynamics) analysis, and the density of protected fragments quantitated at the Fred Hutchinson Cancer Research Center.

In situ hybridization

Frozen embryos were cut into 20 μm sagittal sections on a cryostat, mounted on 3-aminopropyltriethoxysilane-treated slides, processed, hybridized to ^{33}P-labeled sense and antisense 5' probes (see above) and washed as previously described (Wang, Kunkel et

al., 1994). Experiments were also performed using a 3' probe that spans the carboxyl terminus (41 bp of open reading frame and 207 bp of 3' untranslated region).

Slides were apposed to Hyperfilm β-max (Amersham) for 5-6 days to generate autoradiographs, then coated with Kodak NBT-2 emulsion, stored at 4 ^{0}C for 10-12 days, developed, and counterstained with hematoxylin.

Autoradiographic film images were enlarged and digitized using a Dage CCD 72 camera, a Macintosh IIci computer, and the public domain program NIH Image. Final images were generated using a Power Macintosh 8500 and Deneba Canvas™ software. Darkfield images of emulsion-coated slides were collected using NIH Image, a Nikon Optiphot microscope and a Sony CCD-IRIS video camera, and final images generated using Adobe Photoshop™ and Deneba Canvas™ software. Digital images were printed using the Tektronix Phaser II SD dye sublimation system.

Immunocytochemistry (ICC).

Fixed embryos were cryoprotected in sucrose, frozen in embedding medium, cut in 10-20 μm sagittal sections on a cryostat, and affixed to chrome alum-treated slides. ICC was performed according to Wang (Wang, Kunkel et al., 1993) and sections were incubated with the following primary antibodies for 3 days at 4 ^{0}C: polyclonal anti-Kv1.1 at 1:25 (Wang, Kunkel et al., 1993); monoclonal TuJ1 antibody against neuron-specific class III β-tubulin at 1:500 (Moody, Quigg et al., 1989; Easter, Ross et al., 1993); monoclonal 40E-C antibody against vimentin at 1:25 (Alvarez-Buylla, Buskirk et al., 1987); monoclonal RC-2 antibody specific for radial glia at 1:1 (Misson, Edwards et al., 1988); polyclonal anti-Krox-20 at 1:50 (Goddard, Rossel et al., 1996) (Berkeley Antibody Co.); monoclonal anti-GAP-43 at 1:2000 (Goslin, Schreyer et al., 1990). Double staining with anti-Kv1.1 in combination with monoclonal antibodies (TuJ1, 40E-C, RC-2, GAP-43) was performed by coincubation with both primary antibodies.

Double staining with anti-Kv1.1 and anti-Krox-20 (both polyclonal) antibodies was performed using sequential incubations, separated by a blocking step using goat-anti-rabbit IgG $F(ab')_2$ fragments (Jackson Immunoresearch) at 6 ng/μl. Incubation with fluorescent secondary antibodies was simultaneous or sequential as described above and utilized fluorescein- or Texas red-conjugated goat anti-rabbit IgG for polyclonal primary antibodies, or goat anti-mouse IgG and IgM for monoclonal primary antibodies (Jackson Immunoresearch) at 7.5 ng/μl.

Images were collected on a Bio-Rad MRC 1024 scanning laser confocal microscope (V. M. Bloedel Center), processed using Adobe Photoshop™ and Deneba Canvas™ software, and printed using the Tektronix Phaser II SD dye sublimation system.

Results

Kv1.1 transcript levels are temporally regulated during murine development

To determine if Kv1.1 is expressed during murine embryonic development and if its expression is developmentally regulated in mice, RNase protection assays were performed, comparing Kv1.1 RNA levels in whole embryos from E9.5 through E16.5. Three separate experiments were performed, using independently isolated tissue samples to generate three different RNA preparations at each embryonic day. The level of Kv1.1 RNA relative to that of 18S ribosomal RNA in each sample was calculated by PhosphorImager quantitation of protected fragments. Kv1.1 transcript levels were relatively high at E9.5 and E14.5, with lower expression at interim stages (Figure 1A and B). Kv1.1 RNA levels were only slightly lower at E8.5 than at E9.5 (n=3, data not shown).

To determine if Kv1.1 expression is also regulated during postnatal development, similar RNase protection assays were performed comparing transcript levels in whole

brain at regular intervals from E17.5 through postnatal day 21 (P21). Three independent experiments detected lowest Kv1.1 expression around the time of birth, gradually increasing levels over approximately 2 weeks, and a dramatic upregulation of expression at about 2 weeks of age (Figure 1C and D).

These results demonstrate that Kv1.1 RNA is expressed during murine embryonic development, and that RNA levels are regulated in a complex temporal pattern. There are two major peaks of expression during embryonic development, followed by an abrupt increase during the second postnatal week that is sustained through adult life.

Kv1.1 RNA decreases from E9.5 to E10.5

To examine the tissue-specific changes in Kv1.1 transcript levels between E9.5 and E10.5, we performed *in situ* hybridization studies using sagitally sectioned embryos. Two separate experiments using 5-10 embryos at each age were performed. At E9.5, Kv1.1 signal was strong in regions of the diencephalon (thalamus and hypothalamus), tectum of the mesencephalon (and tegmentum, data not shown), and in two broad dorsal stripes in the region of the rhombomeres (Figure 2A and B). By E10.5, we no longer detected Kv1.1 signal in the rhombencephalon, and signal density was significantly lower in the mesencephalon (Figure 2C and D). Similar results were obtained with both 5' and 3' riboprobes. These data indicate that Kv1.1 expression at E9.5 is transient, confirming the dramatic decrease in Kv1.1 transcript levels from E9.5 to E10.5 that was detected by RNase protection.

Cellular localization of Kv1.1 at E9.5/E10.5

Fluorescent immunocytochemistry (ICC) experiments using polyclonal antibodies specific to Kv1.1 confirmed the expression pattern observed by *in situ* hybridization. A minimum of two experiments using 5-10 embryos at each age were performed. Strong

Kv1.1 immunoreactivity was detected in two rhombomeres (Figure 3A) as well as in the mesencephalon (Figure 3F). By E10.5, no Kv1.1 immunoreactivity was detected in the rhombomeres (Figure 3B), and staining was substantially lower in regions of the diencephalon and mesencephalon that exhibited staining at E9.5 (data not shown).

To identify the cell types expressing Kv1.1 at E9.5 and throughout embryonic development, we performed double-label ICC for Kv1.1 and specific cellular markers. While expression of markers used throughout this study is developmentally regulated, each was used at a period in development when its expression has been characterized previously and shown to be localized to the specific cell types identified in this study. Thus, to identify the specific rhombomeres expressing Kv1.1, sections were double-labeled with anti-Kv1.1 and antibodies to Krox-20, a zinc-finger transcription factor which localizes to rhombomeres 3 and 5 at E9.5 (Wilkinson, Bhatt et al., 1989). Colabeling identified the two regions of Kv1.1 expression in the hindbrain as rhombomeres 3 and 5 (Figure 3C). The subcellular localizations of Kv1.1 and Krox-20 within the rhombomeres were not identical (Figure 3D), as would be expected since Krox-20 is a transcription factor, and thus might reasonably be found in the nucleus, while Kv1.1 appears cytoplasmic or associated with the plasma membrane.

To address the question of whether Kv1.1 staining at E9.5 is in neurons, sections were double stained with antibodies to Kv1.1 and TuJ1, a neuron specific class III β tubulin, as a marker of early neuronal development (Moody, Quigg et al., 1989; Easter, Ross et al., 1993). In the hindbrain, the two proteins were found in alternating compartments, and only cells positive for TuJ1 had distinct neuronal morphologies (Figure 3E). Kv1.1 and TuJ1 proteins also failed to colocalize in the E9.5 mesencephalon (Figure 3F), where Kv1.1 staining was strongest in the ventricular, or proliferating zone, while TuJ1 immunoreactivity was observed mainly in the differentiating field. In the ventricular zone, Kv1.1 staining was robust in large branched cells with endfeet at the

edge of the ventricle (Figure 3F). Double labeling with anti-Kv1.1 and RC-2, a marker specific for radial glia (Misson, Edwards et al., 1988), detected both proteins in these branched cells in the ventricular zone (Figure 3G). The location, morphology and RC-2 immunoreactivity indicate these cells are radial glia. Collectively, these data indicate that at E9.5, Kv1.1 is not found in cells that are differentiated neurons, but is found in a population of early glial cells.

Kv1.1 RNA peaks transiently around E14.5

In situ hybridization experiments using sectioned embryos were performed to examine the tissue-specific expression of Kv1.1 between E14.5 and E17.5. At E14.5, Kv1.1 transcripts were widespread in both the developing central (CNS) and peripheral nervous systems (PNS), with particularly strong expression in sensory structures (Figure 4A and B, Table 1). By E17.5, Kv1.1 signal was significantly lower in the CNS, but still relatively high in sensory ganglia (Figure 4C and D, Table 1). These experiments confirm the decrease in Kv1.1 expression from E14.5 to E17.5 that was detected by RNase protection, and demonstrate that, in some CNS structures, there is a second period of transient Kv1.1 expression during mouse development. Interestingly, Kv1.1 RNA was detected along the pathways of several peripheral nerves at both E14.5 and E17.5, suggesting its presence in either glia or axons.

Cellular localization of Kv1.1 at E14.5/E15.5

Because Kv1.1 expression is so widespread at E14.5, we have focused our tissue-specific examination of expression on three regions of the nervous system: 1) cortex and hippocampus; 2) DRG and peripheral nerves; and 3) trigeminal ganglion and nerve. Each of these regions gives rise to both neurons and glia, but each has a different embryonic origin; the cortex and hippocampus are derived primarily from neural ectoderm, the DRG

from primarily neural crest cells, and the trigeminal ganglion from both neural crest and placodal cells (reviewed in (Jacobson, 1991). Despite having different embryonic origins, the results for each region are similar; namely, that Kv1.1 appears in a subset of neurons as well as a subset of non-neuronal cells. In most cases, these non-neuronal cells were identified as glia, based on location, morphology and staining with antibodies to either vimentin, RC2, or Krox-20.

Cortex and hippocampus

At E14.5, Kv1.1 RNA hybridization signal was strong in the cortex and hippocampus, appearing predominantly in the outer aspects or differentiating fields (Figure 5A). Kv1.1 protein was also detected in the cortical and hippocampal differentiating fields, and immunostaining was very robust in large individual cells within the subventricular zone (Figure 5B and C). Double staining ICC experiments demonstrated some overlap in Kv1.1 and TuJ1 immunoreactivities in the differentiating fields (Figure 5D), while the cells in the subventricular zone exhibited either Kv1.1 or TuJ1 staining, but not both (Figure 5E). In some instances, TuJ1-positive cells were located immediately adjacent to cells with Kv1.1 immunoreactivity, suggesting the Kv1.1-positive cells in the subventricular zone were radial glia. ICC experiments were performed using two glial markers: vimentin, which is expressed in radial glia and glial precursors (Alvarez-Buylla, Buskirk et al., 1987); and RC2, a marker specific for radial glia (Misson, Edwards et al., 1988). Both vimentin (Figure 5E) and RC-2 (Figure 5F) immunoreactivities were found in cells with Kv1.1 protein, indicating that Kv1.1 is expressed in radial glia and possibly glial precursors. Interestingly, Kv1.1 was found only in a subset of cells positive for RC-2. These data indicate that in the E14.5 cortex and hippocampus, Kv1.1 is expressed in a subset of both neurons and glia.

DRG and peripheral nerves

At E14.5, Kv1.1 RNA expression was robust in a subset of cells in the DRG (Figure 6A), and was also detected along the pathways of peripheral nerves (Figure 4A). ICC experiments confirmed the expression of Kv1.1 protein in only a subset of ganglion neuron somata, and also revealed a population of small, rounded cells adjacent to sensory ganglia and along peripheral nerves with very robust Kv1.1 immunoreactivity (Figure 6B). Colabeling studies using anti-Kv1.1 and either of two early neuronal markers, TuJ1 (Moody, Quigg et al., 1989; Easter, Ross et al., 1993) or GAP-43 (Goslin, Schreyer et al., 1990), showed that Kv1.1 is expressed in neurons with at least two sizes of cell bodies and that the adjacent Kv1.1-expressing cells are not neuronal somata or axons (Figure 6C and D). Because sensory ganglion neurons are sometimes classified based on differences in somata size (reviewed in (Kai, 1989; Carr and Nagy, 1993), the presence of Kv1.1 protein in multiple sizes of neurons suggests this channel may be expressed in multiple neuronal populations within the ganglia.

Krox-20, which is not specific for glial cells, but is found in both sensory ganglia and glial precursors at E14.5/15.5 (Topilko, Schneider et al., 1994), was used as a marker for glial cells. At both E14.5 and E15.5, we found the Krox-20 staining pattern to be as previously reported, and found Kv1.1 and Krox-20 staining patterns overlapped in the small cells adjacent to sensory ganglia (Figure 6E) and peripheral nerves (Figure 6F-I). Based on their location, morphology and Krox-20 immunoreactivity, we identify the non-neuronal cells expressing Kv1.1 that are adjacent to sensory ganglia as their glial components (called satellite or boundary cap cells), and those along the pathway of peripheral nerves as Schwann cell precursors.

Trigeminal ganglion and nerve

At E14.5, the trigeminal ganglion displayed very robust Kv1.1 hybridization signal, with Kv1.1 RNA being detected along the pathways of all three branches of the trigeminal nerve (Figure 7A). Kv1.1 immunoreactivity was also strong in the trigeminal

ganglion and along the trigeminal nerves (Figure 7B). There was a substantial overlap in Kv1.1 and TuJ1 staining in the ganglia and nerve fibers as they exit the ganglia (Figure 7C-E), but some cells adjacent to the ganglia and those along the pathway of peripheral nerves expressed only Kv1.1 (data not shown, see similar results in DRG). Within the trigeminal ganglion, Kv1.1 was found in neuronal cell bodies of three distinct sizes (Figure 7F), again suggesting that Kv1.1 might be localized to multiple neuronal populations in the ganglia. These data indicate that Kv1.1 is present in both the somata and axons of most trigeminal neurons, and also in glial cells associated with the axons or ganglia.

Collectively, these data demonstrate that Kv1.1 is expressed in cells with both neuronal and non-neuronal phenotypes at E14.5, and that the non-neuronal cells include multiple populations of glial cells.

Discussion

We find that the expression of Kv1.1 undergoes a multiphasic, tissue-specific pattern of regulation during murine development. The same changes in expression were detected using three separate methods: RNase protection, *in situ* hybridization, and immunocytochemistry. In the embryo, there are two transient peaks of Kv1.1 expression: at E9.5 and E14.5. The first and most tightly regulated expression of Kv1.1 at E9.5 appears to occur primarily in non-neuronal cells. Expression of Kv1.1 does not appear in neuronal cells until the second phase of Kv1.1 expression, which peaks at E14.5. The pattern of murine Kv1.1 expression at E14.5 is strikingly similar to the xKv1.1 pattern detected in stage 42 *Xenopus* embryos (Ribera and Nguyen, 1993). In both mice and amphibians, Kv1.1 message is found in both the CNS and PNS, where it localizes to areas with significant contributions from neural crest cells , including the trigeminal ganglion, spinal ganglia, and glial cells. Thus, the peak of Kv1.1 expression at

E14.5 in mouse may reflect similar developmental events related to neural crest development that are conserved in amphibians and mammals.

The (E14.5) embryonic versus the adult distributions of Kv1.1 can be related in only a subset of the tissues examined here. In peripheral nerves, Kv1.1 is strongly expressed at E14.5, and strong expression continues through adult life; however, the punctate pattern of staining seen in the adult (Wang, Kunkel et al., 1993) is not apparent at E14.5. Within the CNS, neurons occupying similar regions express Kv1.1 in both embryos and adults, but because the expression at E14.5 is transient, it is uncertain if the adult expression occurs in the same cells as in the embryo. In glial cells, Kv1.1 expression is quite different in 14.5 day embryos and adults. We have demonstrated robust Kv1.1 expression in several embryonic glial populations, while in the adult, Kv1.1 is only weakly detected in mature astrocytes (Smart, Bosma et al., 1997), and mature Schwann cells (Mi, Deerinck et al., 1995). Also, the subcellular localization of Kv1.1 appears to differ in embryonic and in mature Schwann cells, with strong, diffuse expression in the embryo versus an exclusively perinuclear localization in mature Schwann cells. Thus, while the cellular patterns of Kv1.1 expression can be correlated between embryo and adult, the level of expression and subcellular localization usually differ.

Postnatally, expression of Kv1.1 in the CNS is low at birth (P0), and rises dramatically at the end of the second postnatal week (P12-P15). This postnatal upregulation immediately precedes the onset of a seizure phenotype in Kv1.1-null mice (Smart, Lopantsev et al., 1998) suggesting that the seizure phenotype in Kv1.1-null mutants is due at least in part to functional deficiencies in mature neurons.

Our results show that dramatic changes in Kv1.1 RNA and protein levels can occur over 24 hours, suggesting that both Kv1.1 message and protein are labile and turnover is tightly regulated. In addition, we found that the tissues with the highest Kv1.1 transcript levels also exhibit the strongest Kv1.1 immunoreactivity. This is consistent with others'

findings that the development of I_{Kv} in *Xenopus* neurons requires a period of new RNA synthesis (Ribera and Spitzer, 1989), and coincides with increasing xKv1.1 transcript levels (Gurantz, Ribera et al., 1996).

Potential functions of Kv1.1 during development

In mature neurons, the functions of voltage-gated K^+ currents have been studied extensively. Delayed rectifier currents (to which Kv1.1 is thought to contribute) repolarize axons following action potentials, and in this way are thought to regulate neuronal excitability (Hille, 1992). While our studies do not directly assess the developmental roles of Kv1.1, several factors suggest this channel may serve different functions in embryos than in mature neurons. First, Kv1.1 is expressed at very early stages of nervous system development, prior to the extension of neurites or the establishment of synaptic connections in many cells expressing Kv1.1. Second, Kv1.1 is strongly expressed in non-neuronal (including glial) cells in the embryo. Finally, the tightly regulated, transient expression of Kv1.1 in embryos suggests this channel is involved in developmental processes that occur only at specific times in embryogenesis.

By what mechanism(s) might a Kv channel influence cellular processes involved in development? The simplest explanation is that, by influencing resting membrane potential or repolarization rates, Kv1.1 regulates calcium influx, thereby affecting calcium-sensitive processes such as protein phosphorylation, changes in gene expression and release of intercellular signaling molecules. Several developmental processes are known to be influenced by the amount or rate of calcium influx into cells, including neuronal cell migration (Rakic and Komuro, 1995, Goldman, 1996 #69; Komuro and Rakic, 1996), growth cone migration (Cohan, Connor et al., 1987; Neely and Gesemann, 1994; Williams and Cohan, 1995), Schwann cell migration (Letourneau, Roche et al., 1991; Anton, Hadjiargyrou et al., 1995), cell-cell adhesion (reviewed in (Damsky, Sutherland et al.,

1993; Marrs and Nelson, 1996), and neuronal differentiation (reviewed in (Moody, Simoncini et al., 1991; Emerit, Riad et al., 1992; Finkbeiner and Greenberg, 1996). While calcium-dependent mechanisms are well established, it is possible that Kv1.1 expression may affect transduction of other developmental signals or may be involved in direct cell-cell recognition.

Possible cellular processes regulated by Kv1.1

When one considers the tissue- or cell-specific localization of Kv1.1, the timing of its expression, and our current knowledge of the cellular processes taking place in tissues or cells expressing Kv1.1 during development, there is evidence to support roles for Kv1.1 in at least three distinct cellular processes: cell-cell adhesion; migration; and proliferation.

Kv1.1 might play a role in cell-cell adhesion in the rhombomeres, which are periodic bulges in developing vertebrate hindbrains that underlie the segmental patterning of the hindbrain, and delineate molecular compartments of restricted gene expression (reviewed in (Nieto, Bradley et al., 1992). Pairs of rhombomeres give rise to associated sensory ganglia, brachiomotor nerves, and other neural crest derivatives such as glia, bone, cartilage, and pigment epithelium (reviewed in (Lumsden and Keynes, 1989)). For example, rhombomeres 2 and 3 give rise to the trigeminal ganglion, motor roots of the trigeminal nerve, and associated glial components, while rhombomeres 4 and 5 give rise to the facial/vestibular ganglion, its motor roots, and glia. In chick embryos, clonal analysis indicates that only a minor degree of cellular mixing occurs between rhombomeres (Fraser, Keynes et al., 1990), and rhombomeres also exhibit differential adhesiveness that is cadherin-mediated (Guthrie, Prince et al., 1993; Wizenmann and Lumsden, 1997), suggesting there may be differential expression or regulation of cell adhesion molecules in alternating rhombomeres. Cadherins are a large family of calcium-dependent adhesions

molecules that mediate homophilic interactions between cells (reviewed in (Grunwald, 1993), and their adhesive function appears to be regulated by reversible phosphorylation of cadherin-associated molecules which may involve protein kinase C (reviewed in (Nagafuchi, Tsukita et al., 1993). At least one member of this family, cadherin 6, has been found to be expressed in a rhombomere-restricted pattern at E9.5 (Inoue, Chisaka et al., 1997). Our finding that Kv1.1 is broadly expressed in rhombomeres 3 and 5 at E9.5 suggests that Kv1.1 might influence cell-cell adhesion within these rhombomeres, perhaps by regulating the calcium-sensitive phosphorylation of cytoplasmic molecules that interact with cadherins.

Several lines of evidence suggest Kv1.1 might play a role in migration. First, Kv1.1 is expressed in several cell types that are migratory or involved in migration. At both E9.5 and E14.5, Kv1.1 is strongly expressed in radial glia, which provide the scaffolding for migration of proliferating progenitors and newly differentiated neurons in the developing CNS (reviewed in (Jacobson, 1991). At E14.5, Kv1.1 is found in the axons of peripheral nerves and in Schwann cell precursors, which migrate into the periphery along these axons (reviewed in (Jacobson, 1991). Second, migration of neurons, glia and growth cones have all been shown to be regulated by calcium influx, which we have suggested could be regulated by Kv channel expression. Interestingly, the cadherin family of adhesion molecules has also been shown to be involved in the migration of growth cones (Letourneau, Shattuck et al., 1990) and Schwann cells (Letourneau, Roche et al., 1991) to their peripheral targets, suggesting Kv1.1 might influence migration by regulating the calcium-sensitive phosphorylation of molecules that interact with these cell adhesion molecules. Finally, *weaver* mutant mice, which have a deficit in the movement of a subset of cerebellar neurons to their adult locations (Hatten, Liem et al., 1986; Maricich, Soha et al., 1997), have a mutation in another K^+ channel, the G-protein coupled inward rectifier GIRK2 (Patil, Cox et al., 1995). While the mechanism

responsible for the migratory deficit is not understood, these findings indicate the GIRK2 is required for the normal migration of these neurons, and are consistent with the idea that other K^+ channels might also be involved in neuronal migration.

There is substantial evidence suggesting Kv1.1 plays a role in Schwann cell proliferation. First, cultured postnatal Schwann cells express a delayed rectifier current, increases in current density parallel proliferation in the Schwann cells, and blockade of I_{Kv} inhibits their proliferation (Wilson and Chiu, 1993). Second, Kv1.1 is expressed in proliferating cultured Schwann cells, and its expression and I_{Kv} current density are downregulated as cells stop proliferating and begin differentiating (Chiu and Wilson, 1989; Chiu, Scherer et al., 1994). Third, in the dysmyelinating mouse mutant *shiverer*, there is an approximately 2-fold increase in the number of CNS glia, as well as an approximately 4-fold increase in Kv1.1 expression in individual glial cells (Wang, Allen et al., 1995). Fourth, C6 glioma cells, a cultured cell line that is often used to study glial differentiation, express Kv1.1 (Wang, Castle et al., 1992). Strong Kv1.1 expression appears to be the major determinant of the resting membrane potential in undifferentiated C6 glioma cells, and pharmacological treatments that induce a decrease in Kv1.1 RNA levels also inhibit proliferation (Allen, Koh et al., 1998). Our finding that Kv1.1 is strongly expressed in glia and glial precursors during development is consistent with a potential role for this channel in glial proliferation *in vivo*.

Thus, there are multiple developmental processes in which Kv1.1 might be involved. Our results suggest that the expression of Kv1.1 in multiple populations of embryonic cells may provide a means for differential regulation of these processes in different populations within the developing mammalian nervous system.

Table 1. Summary of Kv1.1 expression in E14.5 and E17.5 mouse embryos

	E14.5	E17.5
cerebral cortex	+++	+
hippocampus	+++	+
pineal	+++	+
radial glia	+++	++
superior colliculus	++	+
inferior colliculus	++	+
epithalamus	++	-
pituitary	+	-
cranial ganglia (trigeminal, facial, spiral)	+++	+++
dorsal root ganglia	+++	++
thalamus	++	-/+
hypothalamus	++	-
chief sensory and spinal trigeminal nuclei	++	+
medial vestibular nucleus	++	+
satellite cells	+++	+++
Schwann cells/precursors	+++	+++
olfactory epithelium	++	-
epithelium of the tongue	++	-
enteric nervous system	++	??
thymus	+	-

Figure 1. Temporal regulation of Kv1.1 expression. **(A)** Autoradiograph of an RNase protection assay (RPA) gel demonstrating changing Kv1.1 transcript levels from E9.5 through E16.5. In the upper panel, total RNA from adult tissue (liver, brain) or from whole embryos was hybridized to a 310 basepair (bp) ^{32}P-labeled 5' Kv1.1 antisense riboprobe. Following hybridization, RNase digestion produced a 252 bp protected fragment. Below, samples were diluted and hybridized to a 423 bp ^{32}P-labeled 18S ribosomal subunit riboprobe (350 bp protected fragment) to control for the amount of RNA in each sample. Fragment sizes are indicated in basepairs. **(B)** PhosphorImager (PI) analysis of 3 RPA gels using 3 different sets of RNA preparations. Kv1.1 band intensity is expressed as a percentage of corresponding 18S band intensity and plotted on the ordinate vs. embryonic age on the abscissa. Relatively high expression of Kv1.1 is detected at E9.5 and E14.5, separated by a period of lower expression. Error bars indicate standard error. **(C)** Autoradiograph of an RPA gel demonstrating changing Kv1.1 RNA levels in the CNS from E17.5 through P21. Total RNA from whole brains was hybridized to the same probes as in part A. **(D)** PI analysis of 3 RPA gels demonstrating that Kv1.1 RNA levels in whole brain are lowest at about the time of birth, and are dramatically upregulated at about 2 weeks of age. Error bars indicate standard error.

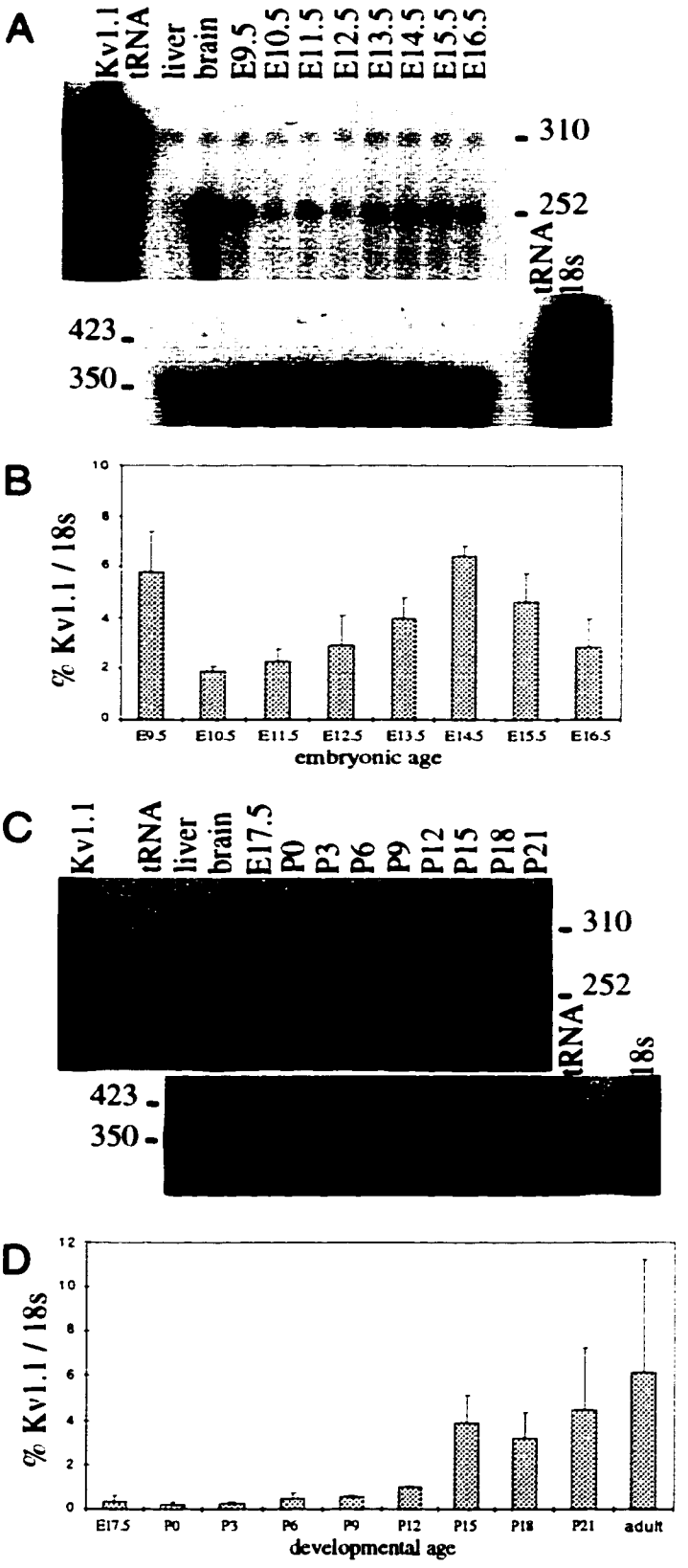
A
Kv1.1
tRNA
liver
brain
E9.5
E10.5
E11.5
E12.5
E13.5
E14.5
E15.5
E16.5
310
252
tRNA
18s
423
350
B
% Kv1.1 / 18s
E9.5
E10.5
E11.5
E12.5
E13.5
E14.5
E15.5
E16.5
embryonic age
C
Kv1.1
tRNA
liver
brain
E17.5
P0
P3
P6
P9
P12
P15
P18
P21
310
252
tRNA
18s
423
350
D
% Kv1.1 / 18s
E17.5
P0
P3
P6
P9
P12
P15
P18
P21
adult
developmental age

Figure 2. Tissue-specific expression of Kv1.1 RNA between E9.5 and E10.5. Note that embryos nearly double in size during this 24 hour period, so only a fraction of an E10.5 embryos is visible in the same size field that shows an entire embryo at E9.5. **(A, B)** Darkfield images generated by *in situ* hybridization of adjacent E9.5 sagittal sections with ^{33}P-labeled 5' Kv1.1 antisense, or hybridizing (A) and sense, or control (B) riboprobes. Strong Kv1.1 expression is found in the diencephalon (Th-thalamus, H-hypothalamus), mesencephalon (Tec-tectum), and in two broad dorsal stripes in the hindbrain (arrows). **(C,D)** Darkfield images of E10.5 sagittal sections hybridized with the same antisense (C) and sense (D) probes as above. The tissue edge is marked with a dashed line. Signal density is significantly diminished in the mesencephalon (tectum-Tec, tegmentum-Teg), and no Kv1.1 RNA is detected in the hindbrain (arrows).

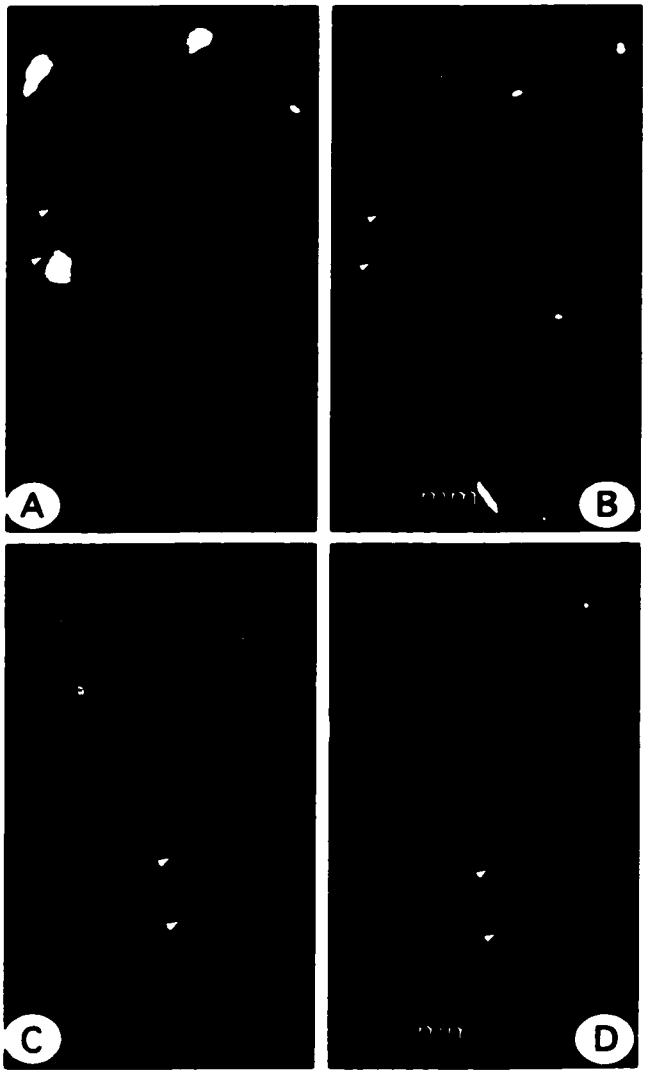
A
B
C
D

Figure 3. Cellular localization of Kv1.1 protein at E9.5/E10.5 using sagittal sections. The orientations are the same for panels A-E, with dorsal (D) to the left and ventral (V) to the right as in panel A. **(A)** Fluorescent immunocytochemistry (ICC) at E9.5 using polyclonal antibodies specific for Kv1.1 and Texas-red conjugated secondary antibodies detects strong Kv1.1 immunostaining in 2 regions of the hindbrain. **(B)** A similar experiment at E10.5 does not detect any Kv1.1 protein in the hindbrain. **(C)** Double staining ICC at E9.5 with anti-Kv1.1 (red) and anti-Krox-20 (green) demonstrating colocalization of both proteins in rhombomeres (r)3 and r5. The tissue in (C) and (D) was exposed to detergent twice as long as tissue in other panels (2 sequential polyclonal antibodies), resulting in decreased membrane integrity and a more diffuse staining pattern with higher background. **(D)** Approximately 6-fold magnification of the boxed area in (C) shows Krox-20 immunoreactivity (green) surrounded by Kv1.1 staining (red). **(E)** Colabeling with anti-Kv1.1 (red) and the early neuronal marker TuJ1 (green) demonstrating that the two proteins are found in alternating rhombomeres, with Kv1.1 in odd numbered (3 and 5) and TuJ1 in even numbered rhombomeres. Because embryos were staged by vaginal plug date and not somite number, the animals used in (A) and (E) are probably at slightly different developmental ages, and the difference in Kv1.1 staining may represent a rostral-caudal gradient that is often observed for molecules with rhombomere-restricted expression. **(F)** Double ICC at E9.5 shows nonoverlapping Kv1.1 (red) and TuJ1 (green) immunoreactivities in the thalamus. Kv1.1 immunoreactivity is robust in large cells with endfeet at the edge of the ventricle (arrows). The ventricle (Vnt) is to the left. **(G)** Colabeling with anti-Kv1.1 (green) and RC-2 (red) demonstrating colocalization of both proteins in branched cells with endfeet at the ventricular edge (arrows).

Figure 4. Tissue-specific changes in Kv1.1 expression between E14.5 and E17.5. **(A,B)** Autoradiographs of adjacent E14.5 sagittal sections hybridized to ^{33}P-labeled 5' Kv1.1 antisense (A) and sense (B) riboprobes to detect Kv1.1-specific signal and background, respectively. Strong Kv1.1 signal is found in both the CNS and PNS, including cerebral cortex (Ctx), hippocampus (Hip), trigeminal ganglion (TG), dorsal root ganglia (DRG), in sensory nuclei of the medulla (large arrows), and along the pathways of peripheral nerves (small, long arrows). **(C, D)** E17.5 sagittal sections hybridized to the same 5' antisense (C) and sense (D) probes as above, demonstrating much lower Kv1.1 signal density in the cortex (Ctx) and hippocampus (Hip), while hybridization signal is still strong in sensory ganglia (TG, DRG) and along the pathways of peripheral nerves (arrows).

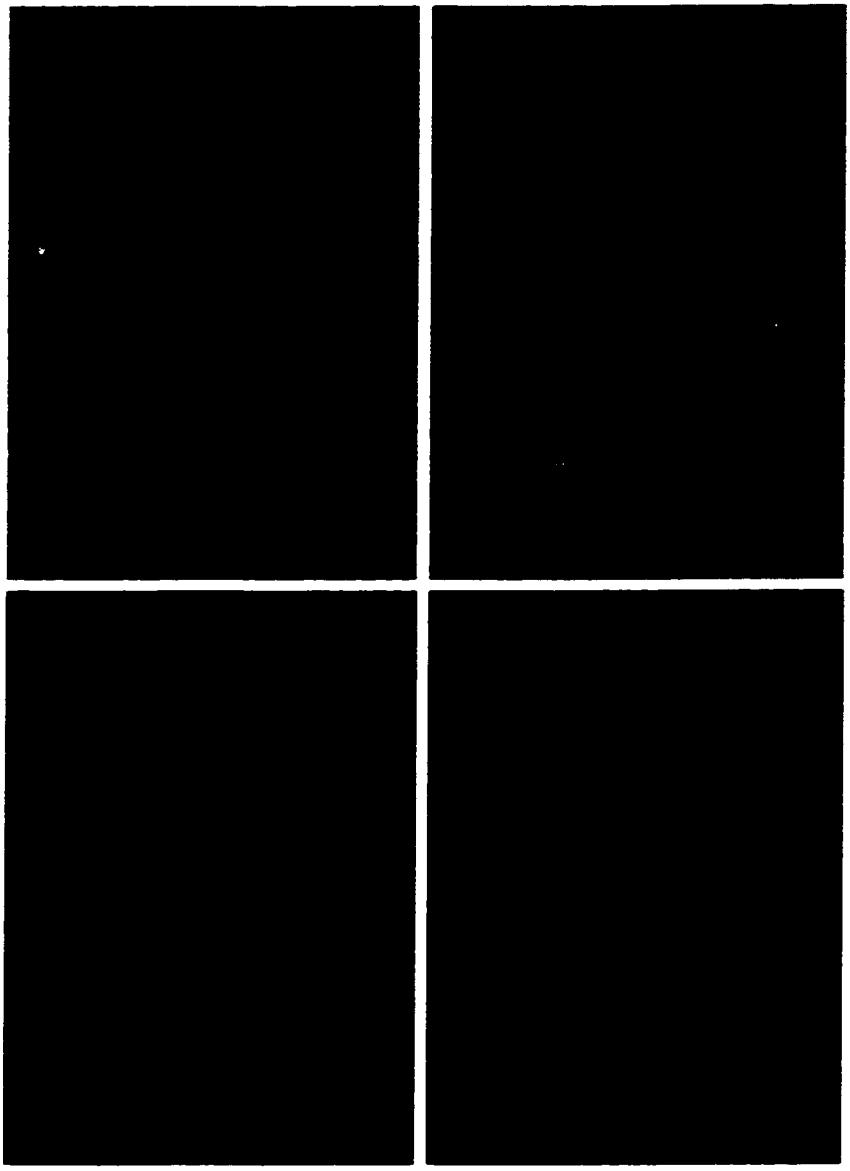

Figure 5. Cellular localization of Kv1.1 in the CNS at E14.5. **(A)** Darkfield image showing strong Kv1.1 hybridization signal in the outer aspects of the cortex (Ctx) and hippocampus (Hip). **(B)** Moderate Kv1.1 immunostaining is found in the outer aspect of the cortex (Ctx), and very robust staining in large cells in the subventricular zone (arrows). The ventricle (Vnt) is to the right, and the ventricular edge marked with a dashed line. **(C)** Magnification of a single large cell positive for Kv1.1 in the subventricular zone of the cortex. **(D)** Colabeling ICC in the hippocampus demonstrating some overlap in Kv1.1 (red) and TuJ1 (green) localization in the differentiating field. **(E)** Double staining ICC in the cortex (cortical plate toward the top and ventricle toward the bottom) shows Kv1.1 (red, small arrow) and TuJ1 (green) proteins are not localized in the same cells in the subventricular zone. A single TuJ1 positive cell (large arrowhead) is seen immediately adjacent to a cell with Kv1.1 staining. **(F)** Colabeling ICC with anti-Kv1.1 (red) and anti-vimentin (green) demonstrating colocalization in large cells in the subventricular zone of the pons. **(G)** Double immunostaining shows Kv1.1 immunoreactivity (green) overlaps with that of RC-2 (red) in some cells in the subventricular zone of the cortex (small arrow), and some cells are positive for RC-2 only (large arrowhead). The ventricle is toward the lower right.

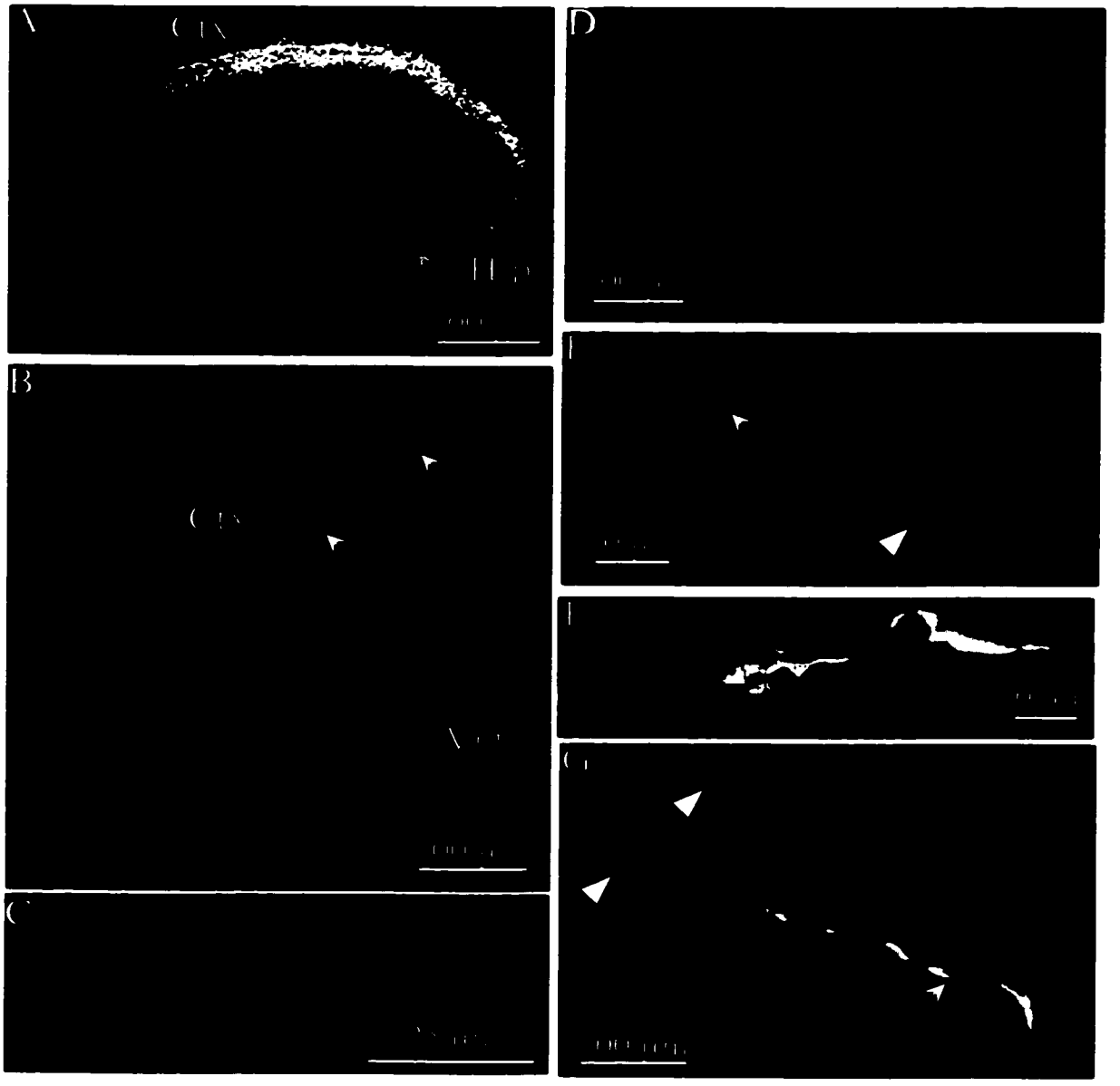

Figure 6. Cellular localization of Kv1.1 in dorsal root ganglia and peripheral nerves at E14.5/E15.5. Panels A-D are from E14.5 embryos, and panels E-H are from E15.5 embryos. **(A)** Darkfield image showing strong Kv1.1 hybridization signal in a subset of cells in the dorsal root ganglia (large arrowhead). Kv1.1 signal is also detected in nearby bone and cartilage (small arrow), but it is unlikely this signal is specific for Kv1.1, because it did not develop in all experiments, and strong background signal developed in bone using the control probe in a portion of experiments. **(B)** ICC detects strong Kv1.1 staining in some cells of the dorsal root ganglia, and very robust immunoreactivity in cells along the emerging nerve fibers (arrow). **(C)** Colabeling ICC with anti-Kv1.1 (red) and TuJ1 (green) shows localization of both proteins in two sizes of neurons (S-small and L-large) in the ganglia (large arrowheads), while only Kv1.1 immunoreactivity is seen in the small cells adjacent to the ganglion (small arrows). **(D)** Double immunolabeling with anti-Kv1.1 (green) and anti-GAP-43 (red), an axonal marker, shows both proteins in peripheral axons, and only Kv1.1 staining in small cells adjacent to the axons (arrows). **(E)** Double immunostaining with Kv1.1 (red) and Krox-20 (green) demonstrating localization of both proteins in the small, rounded cells adjacent to sensory ganglia. **(F-H)** Colabeling ICC with anti-Kv1.1 (red) and anti-Krox-20 (green) at E15.5 demonstrating colocalization of both proteins in small cells adjacent to a peripheral nerve. (E) is a low-magnification image showing a large section of nerve. (F) is an approximately 5-fold magnification of the boxed area in (E).

Figure 7. Cellular localization of Kv1.1 in the trigeminal ganglion and nerve at E14.5. **(A)** Darkfield image exhibiting strong Kv1.1 hybridization signal in cell bodies of the trigeminal ganglion (TG) and along the pathways of all three branches of the trigeminal nerve, or the ophthalmic (Opt), maxillary (Max) and mandibular (Mand) nerves. Signal was also detected in nearby bone and cartilage (small arrows), but is probably not specific signal (see Figure 6A). **(B)** Robust Kv1.1 immunostaining in the trigeminal ganglion and along emerging nerve fibers. **(C-E)** Double immunofluorescent staining with anti-Kv1.1 (red) and the early neuronal marker TuJ1 (green) demonstrating substantial, but not complete, colocalization of both proteins in cell bodies in the trigeminal ganglion and in emerging axons. **(F)** Kv1.1 immunoreactivity in three different sizes of neuronal cell bodies in the trigeminal ganglion (I-intermediate, L-large, S-small).

CHAPTER 3: EXPRESSION OF OTHER SHAKER-LIKE Kv CHANNELS DURING EMBRYONIC DEVELOPMENT

Introduction

Several factors suggest possible functional redundancy among different α subunits of Kv channels. First, similar gating and kinetic properties result in similar currents over at least some membrane potentials. For example, Kv1.1 and Kv1.2 exhibit a 10-30 mV difference in the voltage of activation when expressed alone in exogenous expression systems, but both channels give rise to slowly inactivating outward currents (Stuhmer, Stocker et al., 1988; Bosma, Allen et al., 1993; Hopkins, Allen et al., 1994). Second, the overlapping patterns of channel distribution are consistent with multiple channels contributing to functionally similar currents. For example, both Kv1.1 and Kv1.2 channels are clustered in juxtaparanodal regions of myelinated axons where they appear to have similar functions (Wang, Kunkel et al., 1993; Rasband, Trimmer et al., 1998; Vabnick, Trimmer et al., 1999). Finally, the ability of α subunits from within a given subfamily to coassemble into functional channels suggests that the presence of other subunits may partially or completely compensate for a deficiency of a single subunit type. This possible redundancy makes it difficult to assign a particular physiological function to a given channel subunit. Additionally, the functional roles of channel subunits may vary at different times in development.

To avoid the issue of possible redundancy, we wanted to determine if any region exclusively expresses Kv1.1 as the only Shaker-like Kv channel subunit during embryonic development. Hence, we performed ICC with antibodies specific to Kv1.1 and other individual Shaker-like channel subunits (Kv1.2-1.6) during the two peaks in Kv1.1 expression, namely E9.5 and E14.5.

Materials and Methods

Animals

See Chapter 2.

Immunocytochemistry

ICC was performed as in Chapter 2, and 10-20 μm sagittal E9.5 and E14.5 cryostat sections were incubated with the following antibodies at the indicated dilutions for 20-40 hours: polyclonal anti-Kv1.1 at 1:25 (Wang, Kunkel et al., 1993); polyclonal anti-Kv1.2 at 1:500 (Rhodes, Keilbaugh et al., 1995) (gift of J. Trimmer, State University of New York at Stonnybrook, Long Island, NY); monoclonal anti-Kv1.4 at 1:600 (Rhodes, Keilbaugh et al., 1995) (gift of J. Trimmer); monoclonal anti-Kv1.5 at 1:500 (Mi, Deerinck et al., 1995) (gift of T. Schwarz, Stanford University, Stanford, CA); monoclonal anti-Kv1.6 at 1:600 (Rhodes, Keilbaugh et al., 1995) (gift of J. Trimmer). Following washes in TBS, sections were incubated with goat anti-rabbit IgG (polyclonal) and goat anti-mouse IgG (monoclonal) secondary antibodies conjugated to fluorescein or Texas Red (Jackson ImmunoResearch) at 6ng/μl or to Alexa 488 or Alexa 594 (Molecular Probes) at a dilution of 1:500.

Images were collected on a Bio-Rad MRC 1024 scanning laser confocal microscope, processed using Adobe Photoshop and Deneba Canvas software, and printed using the Tektronix Phaser II SD dye sublimation system or an Epson Stylus 3000 Inkjet color printer.

Results

Localization of Shaker-like channel protein in embryos

Antibodies specific to Kv1.1, 1.2, 1.4, 1.5 and 1.6 were used to characterize the distribution of these channel subunits in sagittal sections of E9.5 and E14.5 embryos. We did not use antibodies specific for Kv1.3 because this channel is not found at significant levels in adult mouse CNS (Beckh and Pongs, 1990; Grissmer, Dethlefs et al., 1990; Swanson, 1990). Results of this study are presented in figures 8 and 9, and summarized in table 2.

At E9.5, Kv1.1 protein was detected in the same restricted pattern as previously reported in chapter 2, including the tectum shown here (figure 8a). In contrast, Kv1.2 protein was distributed throughout the CNS anlage at E9.5 in a pattern similar to that depicted here in the tectum (figure 8b); no specific cell types were readily identifiable.

Kv1.4 was detected at lower levels than Kv1.2 throughout the CNS anlage. Additionally, Kv1.4 signal was detected in neurites or axons in the developing thalamus (figure 8c). Kv1.5 was not detected in the CNS, but was found in both the atria and ventricles of the heart (figure 8d). Kv1.6 protein was not detected at E9.5.

At E14.5, Kv1.1, 1.2 and 1.5 proteins were identified in distinct but overlapping patterns in both the CNS and PNS. In the CNS, all three proteins were detected in the medulla (figure 9a-c) and at low levels in the outer aspect of the cortex (data not shown). Kv1.1 staining was moderate in fiber tracts in the medulla, and was also detected in an apparent radial glia cell (figure 9a). Kv1.2 signal was found in the fiber tracts of the medulla as well as in some cell bodies; staining was more robust than Kv1.1 and had a patchy appearance (figure 9b). Kv1.5 was detected in medullary fiber tracts and staining was very robust in rows of bipolar cells running parallel to the fiber tracts (figure 9c). We have tentatively identified these cells with robust Kv1.5 signal as glial cells based on their location and bipolar morphology. In the PNS, all three proteins were also found in DRG and peripheral nerves. Kv1.1 staining was robust in a subset of DRG somata and initial segments, very strong in Schwann cell precursors, and was detected at more moderate levels along the length of peripheral nerves (figure 9d, 9g). Kv1.2 was detected in a larger number of DRG somata and along the length of peripheral nerves, but staining was patchy and not detected in initial segments of DRG axons or Schwann cell precursors (figure 9e, 9h). Kv1.5 was weakly detected in a large number of DRG somata and along peripheral nerves, and robust signal was also found in apparent processes of Schwann cell precursors (figure 9f, 9i). In the CNS at E14.5, Kv1.4 protein was weakly detected in the differentiating field of the cortex and also in individual cells in the subventricular zone which we have tentatively identified as radial glia (figure 9j). Kv1.6 protein was not detected at E14.5.

Discussion

We have shown that the pattern of Kv1.1 localization at E9.5 is unique from the other Shaker-like Kv channels; Kv1.1 is the only subunit whose expression is restricted to

tightly defined regions or segments. These findings suggest that Kv1.1 may be playing a unique developmental role in the E9.5 brain. Unfortunately, we have not examined the expression of Shab-, Shaw- or Shal-like Kv channel subunits, and thus can not rule out similar segmental expression of these other families of channel subunits.

At E14.5, the overlapping patterns of Kv1.1, Kv1.2 and Kv1.5 expression are interesting with respect to both heteromultimer formation and functional redundancy. We have found that these three Kv channel subunits often colocalize to the same subcellular region, such as DRG somata and axons of the medulla and peripheral nerves, suggesting they may form heteromultimers in many of these cells *in vivo* during embryonic development. These data are consistent with the findings of others that Kv1.1 can form heteromultimers with Kv1.2 and Kv1.5 in adult mice (Wang, Kunkel et al., 1993; Scott, Muniz et al., 1994). We have also found instances where two subunits colocalize to the same cell type but with different patterns of staining. For example, both Kv1.1 and Kv1.5 subunits are found in apparent glial cells; however, Kv1.1 signal is strongest in the somata while Kv1.5 immunostaining is concentrated in the processes of these cells. These subcellular localizations in embryonic glial cells are similar to those found in adult glial cells but with certain differences. In mature Schwann cells, which have a drastically different morphology than embryonic precursors, Kv1.1 is weakly expressed in a perinuclear pattern, while Kv1.5 is more strongly expressed at the outer leaflet of the myelin sheath (Mi, Deerinck et al., 1995). Similarly, both Kv1.1 and Kv1.5 are expressed in mature astrocytes, where Kv1.5 immunoreactivity is particularly intense in endfoot processes (Roy, Saal et al., 1996; Smart, Bosma et al., 1997). Thus, it appears that while these Kv channel subunits may form heteromultimers *in vivo*, sorting to different subcellular compartments occurs in some cell types.

Functionally, Kv1.1, Kv1.2 and Kv1.5 all give rise to dsustained outward currents when expressed alone in exogenous systems such as CHO cells or *xenopus* oocytes (Stuhmer, Stocker et al., 1988; Swanson, 1990; Bosma, Allen et al., 1993; Hopkins, Allen et al., 1994; Heinemann, Rettig et al., 1996). Each subunit exhibits differences in voltage-dependence of activation and inactivation, but could be functionally redundant in

many cell types. The overlapping patterns of localization during embryonic development may explain why we have detected no gross developmental deficiencies in either the Kv1.1- or Kv1.2-null mutants (unpublished observations).

While we have begun to examine the developmental expression of Kv channels, their functions in the embryo remain unclear. We have previously suggested that Kv1.1 might be involved in establishing the resting membrane potential or repolarization rates of embryonic cell populations, allowing for differential regulation of developmental processes in various cell types (see chapter 2). The findings presented here are consistent with overlapping functions for Kv1.1, Kv1.2 and Kv1.5 in embryonic tissues, which could provide much more complex and subtle regulation of developmental processes between different cell populations than could be achieved with a single subunit type.

Table 2. Summary of Shaker-like channel subunit localization in E9.5 and E14.5 embryos

	E9.5			E14.5			
	CNS		Other	CNS		PNS	
	Glia	Anlage		Glia	Neurons	Glia	Neurons
Kv1.1	+++ radial glia	+++ segmented		++	++	++	+++
Kv1.2	-	++ patchy		-	+++	-	++ patchy
Kv1.4	-	+ patchy	+ thalamic neurites	++	+	-	+/-
Kv1.5	-	-	+++ heart	+++	++	++	++ patchy
Kv1.6	-	-		-	-	-	-

Figure 8. Localization of Shaker-like Kv channel subunits at E9.5 by fluorescent ICC using sagittal sections. The orientations are the same in A-C, with dorsal to the left and ventral to the right. In figure D, dorsal is to the right. **(A)** Kv1.1 immunostaining is robust in a segment of the tectum of the mesencephalon. Signal is also detected in an apparent radial glia cell (arrow) in this region. **(B)** Kv1.2 protein is detected throughout the anlage of the tectum. **(C)** Kv1.4 signal is weakly detected throughout the tectum, and is also found in neurites in the thalamic region (arrows). **(D)** Kv1.5 immunostaining is detected in cardiac myocytes in both the atria (A) and the ventricles (Vnt).

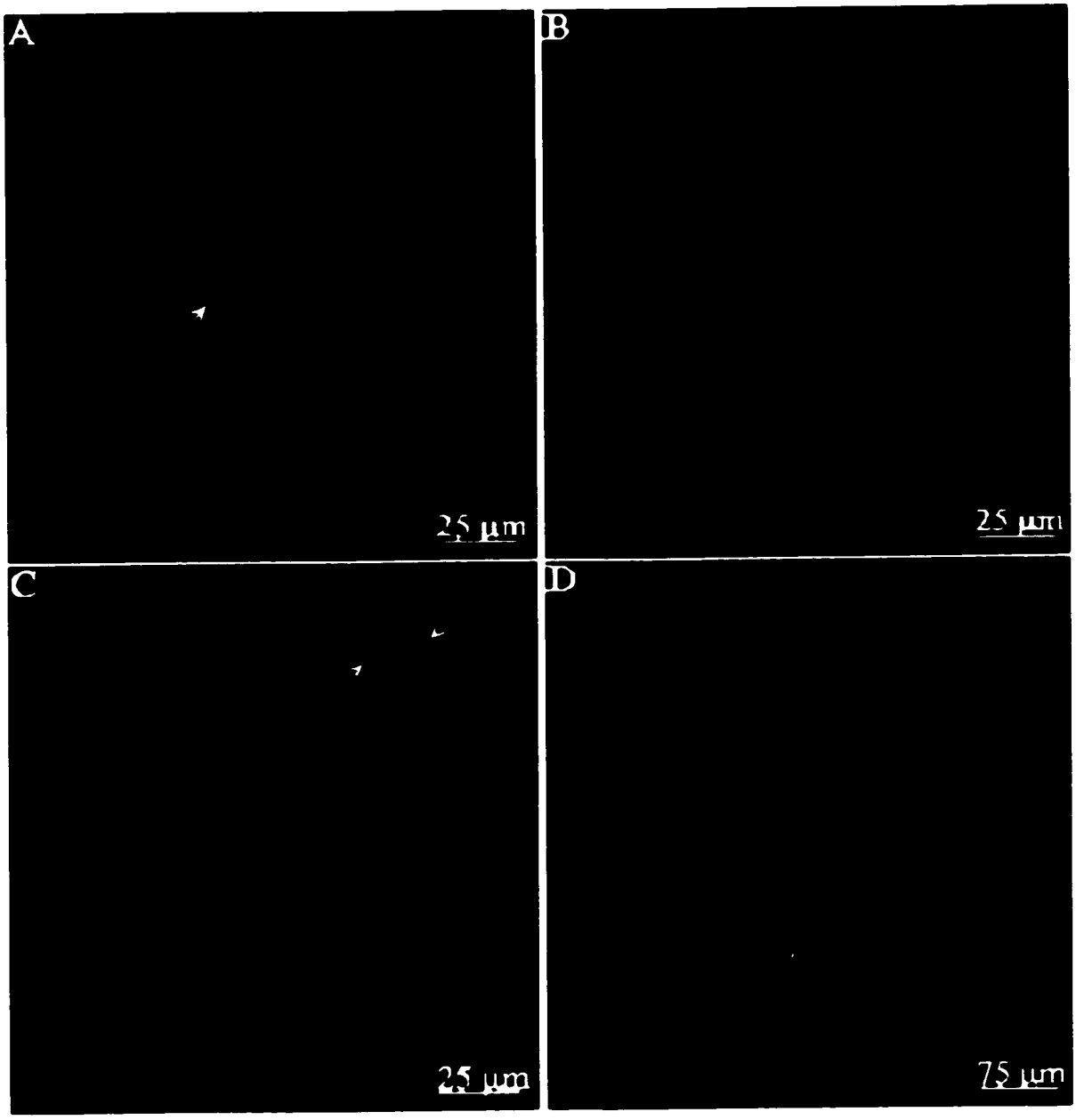
A
25 µm
B
25 µm
C
25 µm
D
75 µm

Figure 9. Localization of Shaker-like channel subunits at E14.5 by fluorescent ICC using sagittal sections. The orientations are the same in A-F, with dorsal to the right and ventral to the left. In G-I, dorsal is to the bottom. In J, dorsal is to the right, and the ventricle is located just below the bottom of the picture. **(A)** Kv1.1 immunostaining in the medulla is weakly detected in fiber tracts (arrowheads) and is more robust in a radial glia cell (arrow). **(B)** Kv1.2 signal in the medulla is robust in fiber tracts (arrowheads) and in cell somata (arrows). **(C)** Kv1.5 protein in the medulla is detected in fiber tracts (arrowheads) and is very robust in rows of bipolar cells that run parallel to the fiber tracts (arrows). **(D)** Kv1.1 signal is robust in a subset of dorsal root ganglion (DRG) somata and emerging axons (arrow) and in satellite glia cells (arrowhead). **(E)** K1.2 protein is found in a large population of DRG somata, but is not readily detected in emerging axons or satellite cells. **(F)** Kv1.5 immunostaining is detected in a large population of DRG somata and is very robust in satellite cells (arrowheads). **(G)** Kv1.1 protein is detected along the length of peripheral axons (arrows) and signal is robust in Schwann cell precursors (arrowhead). **(H)** Kv1.2 signal in peripheral nerves has a punctate appearance and is not detected in Schwann cell precursors. **(I)** Kv1.5 immunostaining is weakly detected along peripheral axons (arrows) and is more robust in processes of Schwann cell precursors (arrowheads). **(J)** Kv1.4 protein is weakly detected in the outer aspect of the cortex (arrows) and in individual cells in the subventricular zone (arrowheads).

CHAPTER 4: THE ROLE OF Kv1.1 IN SCHWANN CELL PROLIFERATION

Introduction

As discussed in chapter 2, there is substantial evidence suggesting Kv1.1 plays a role in glial proliferation. To investigate whether Kv1.1 contributes to the Kv currents regulating Schwann cell proliferation, we have examined the proliferation rates of primary Schwann cell cultures from wildtype (wt; +/+), Kv1.1 heterozygous (het; +/-) and Kv1.1-null or knockout (ko; -/-) congenic littermates under various pharmacological conditions.

Materials and Methods

Animals and Schwann cell cultures

Heterozygous mice lacking one copy of Kv1.1 were generated in our colony and mating pairs or trios established (Smart, Lopantsev et al., 1998). Sciatic nerves were dissected from postnatal day (P) 3 pups born from heterozygous matings and primary Schwann cell cultures established from individual animals. Nerves from individual pups were treated with 0.1% trypsin (Sigma) and 0.1% collagenase (Sigma) in L-15 medium (Sigma), mechanically dissociated with a 23 gauge needle, and plated in individual wells of a 24 well plate in defined medium (Dulbecco's modified eagle medium (GIBCO BRL) containing 10% heat inactivated fetal calf serum (Hyclone), penicillin (50 units/ml), streptomycin (0.05mg/ml) (GIBCO BRL) and 2 mM glutamine (Sigma). 24-36 hours after primary cultures were established, cells were treated for 7-8 hours with the mitotic inhibitor cytosine arabinoside (Sigma) 1 μM to inhibit proliferation of contaminating fibroblasts. Cultures were grown to about 50-70% confluence (5-10 days), pelleted, incubated with 300 μl of an antibody to a fibroblast epitope thy-1.1 at 40 μg/ml (Sigma) in defined medium, then treated with 250 μl rabbit HLA-ABC complement (Sigma) to lyse cells with adherent antibodies. Cells were then resuspended in defined medium, living cells counted on a hemacytometer using trypan blue (Sigma) exclusion, and plated

at 5,000 cells per well in a 96 well plate. Remaining suspended cells were stored at –80 ^{0}C.

At the time of nerve dissection, tails were removed from pups and DNA extracted. Genotyping of tail DNA was performed by PCR using the following primers: Kv1.1 forward-5' TAG CCT CTG ACA GTG ACC TCA GC 3'; neomycin forward-5' CGC CTT CTA TCG CCT TCT TGA CG 3'; common reverse-5' GAA AGC TTC AGG TTC GCC ACT CC 3'. The annealing temperature was 65 °C and the reaction was carried out for 40 cycles. The resulting fragment sizes were 343 bp for the wildtype allele and 481 bp for knockout or neomycin allele. Pups were identified as wt, het, or ko.

Immunocytochemistry

Wildtype Schwann cells (7 days in culture) were grown on microscope slides for ~24 hours, cooled on ice for 10 minutes, medium removed, rinsed with phosphate buffered saline, fixed for 10 minutes in 4% paraformaldehyde, and ICC performed as in chapter 2 with the following primary antibodies at 4 ^{0}C overnight: polyclonal anti-Kv1.1 at 1:25 (Wang, Kunkel et al., 1993); polyclonal anti-Kv1.2 at 1:500 (Rhodes, Keilbaugh et al., 1995) polyclonal anti-Kv1.4 at 1:600 (Rhodes, Keilbaugh et al., 1995); polyclonal anti-Kv1.5 at 1:500 (Mi, Deerinck et al., 1995); monoclonal anti-Kv1.6 at 1:600 (Rhodes, Keilbaugh et al., 1995). Primary antibodies were removed and slides washed with PBS, then incubated with goat anti-rabbit/Alexa 488 (polyclonal) or goat anti-mouse/Alexa 594 (monoclonal) at 1:250 (Molecular Probes). Images were collected, processed and printed as in chapter 3.

Proliferation assays

Triplicate wells of Schwann cells from each individual animal were grown in defined medium, or in the presence of 75ng/ml glial growth factor (GGF; recombinant human heregulin-β1 EGF domain (R&D Systems)) or 10 mM tetraethylammonium (TEA; Kodak) for ~45 hrs. Medium was removed from all wells and plates frozen at –80 ^{0}C. Proliferation assays were performed using the CyQUANT fluorescent system

(Molecular Probes). On the day of the assay, plates were thawed and 200 µl of lysis buffer containing CyQUANT GR fluorescent nucleic acid binding protein was added to each well. A cell number standard curve was generated for each individual culture by plating a dilution series of remaining frozen cells in lysis/fluorescent mix in wells immediately above treated cells. Cell densities were analyzed using a FluorImager 595 and ImageQuant 1.2 (Molecular Dynamics) at the Fred Hutchinson Cancer Research Center (Seattle, WA) and densities converted to cell number based on the standard curves. Data was obtained from 8 (wt and ko) to 9 (het) cultures of each genotype, and the data analyzed using StatView 5.0 (SAS Institute Inc.) and plotted in CA-Cricket Graph III 1.5 (Computer Associates International, Inc.).

Results

Immunocytochemistry

To determine which Shaker-like Kv channels are expressed in our Schwann cell cultures, we performed fluorescent ICC. As shown in figure 10, wildtype Schwann cell cultures express at least four Shaker-like Kv channels: Kv1.1, Kv1.2, Kv1.4 and Kv1.5. Kv1.5 immunostaining was the most robust and was found in both somata and processes; channels were often clustered near the exit point of processes (fig. 10d). Kv1.1 and Kv1.2 signals were of similar intensity, but Kv1.1 was more robust in processes and was often clustered near the exit point of processes (fig. 10a and b). Kv1.4 immunostaining was found only in cell somata and was very patchy in appearance (fig. 10c). Kv1.6 was not detected in our cultures.

Schwann cell proliferation

To determine if Kv1.1 contributes to currents affecting Schwann cell proliferation, we measured cell numbers of wt, het, and ko Schwann cells grown under three culture conditions: untreated (basal proliferation); GGF stimulation; TEA inhibition. A fluorescent image of a plate from a representative assay using cells from four animals in a single litter is depicted in figure 11a; cultured and treated cells were

plated in even numbered rows, and the dilution series used to convert fluorescent density to cell number in odd numbered rows. Cell numbers from triplicate wells were averaged for each culture condition in each animal and plotted in figure 11b. As demonstrated in this individual assay, cell numbers were typically lower in the ko cultures than either the wt or het cultures under all three culture conditions.

The mean cell numbers from each animal of a given genotype were averaged for each culture condition and the results presented in figure 12. Cells of all three genotypes proliferated under basal culture conditions, and proliferation was stimulated by GGF and inhibited by TEA (fig. 12a and b). A one-way analysis of variance did show a significant effect of treatment on overall proliferation rates ($F[2,1.17x10^8)]=74.5$, $p<0.0001$), indicating the sensitivity of our assay was adequate for these experiments.

We detected a consistent trend of decreased proliferation in ko cultures compared to wt and het cultures under all 3 culture conditions (fig. 12a and b). One-way analysis of variance showed that genotype also had a significant effect on overall proliferation rates ($F[2, 2.952x10^7]=8.22$, $p=0.001$). Post-hoc tests (Fisher's least squared difference) revealed a significant difference in overall proliferation rates between wt and ko cultures ($p=0.0035$) and between het and ko cultures ($p=0.0004$).

We also analyzed the data to examine the effect of genotype on each individual culture condition (fig. 12c). One-way analyses of variances did not find a significant effect of genotype on basal ($F[2,1.135x10^7]=2.91$, $p=0.088$), GGF stimulated ($F[2,1.529x10^7)=3.19$, $p=0.072$), or TEA inhibited ($F[2, 5.2x10^6]=2.51$, $p=0.117$) proliferation rates. The lack of significance is probably due in part to the sizeable variability in cell numbers between experiments, as indicated the relatively large standard error bars. It is interesting to note that the decreases in ko proliferation are fairly consistent in each culture condition; cell numbers in ko cultures were consistently between ~75-80% of wt or het cultures.

Discussion

We have shown that Schwann cell cultures express at least four Shaker-like Kv channel subunits: Kv1.1, Kv1.2, Kv1.4 and Kv1.5. The identification of these channel subunits in Schwann cell cultures is consistent with the findings of others indicating there is a diverse and complex repertoire of Kv channels in cultured mouse Schwann cells, which includes α subunits of the Shaker (Kv1.1, Kv1.2, Kv1.4, Kv1.5), Shab (Kv2.1) and Shaw (Kv3.1, Kv3.2) families (Chiu, Scherer et al., 1994; Mi, Deerinck et al., 1995; Sobko, Peretz et al., 1998). Of these four subunits, three of them (Kv1.1, Kv1.2, Kv1.5) give rise to sustained outwardly rectifying K^+ currents when expressed as homomultimers in exogenous expression systems (Stuhmer, Stocker et al., 1988; Swanson, 1990; Bosma, Allen et al., 1993; Hopkins, Allen et al., 1994). These data indicate that all three of these channel subunits could potentially contribute to the Kv currents regulating Schwann cell proliferation.

Schwann cells lacking Kv1.1 were found to have significantly lower overall proliferation rates than either wt or het cultures. This result suggests that Kv1.1 probably contributes to the Kv currents involved in Schwann cell proliferation. The finding that Kv1.1-null Schwann cells are still responsive to the inhibitory effects of TEA blockade indicate that other Kv channel subunits also contribute to these currents.

We also found that proliferation in ko cultures was consistently about 75-80% of either wt or het culture proliferation under all three culture conditions. This finding implies that the proliferative deficit in ko Schwann cells may lie in the basal or intrinsic mechanism of regulation of proliferation, and that equivalent decreases in GGF stimulated or TEA inhibited proliferation merely reflect a smaller base. This might indicate that GGF stimulates a separate or secondary pathway resulting in Schwann cell proliferation.

Collectively, these data indicate that Kv1.1 most likely contributes to the delayed rectifier currents that regulate the intrinsic rate of Schwann cell proliferation, and that other channel subunits, such as Kv1.2 and Kv1.5, may provide some functional redundancy in this role.

Figure 10. Localization of Shaker-like channel subunits in cultured wt Schwann cells by fluorescent ICC. **(A)** Kv1.1 protein was detected in both the somata and processes (arrowhead) of cultured Schwann cells, and channels were often clustered at the exit point of processes from the somata (arrow). **(B)** Kv1.2 signal was readily detected in the somata of cultured Schwann cells, but was less robust in processes. **(C)** Kv1.4 immunostaining was detected in the somata only of cultured Schwann cells, where it had a very patchy appearance. **(D)** Kv1.5 protein was readily detected in the somata and processes (arrowhead) of cultured Schwann cells, and channels were often densely clustered near the exit point of processes from the somata (arrow).

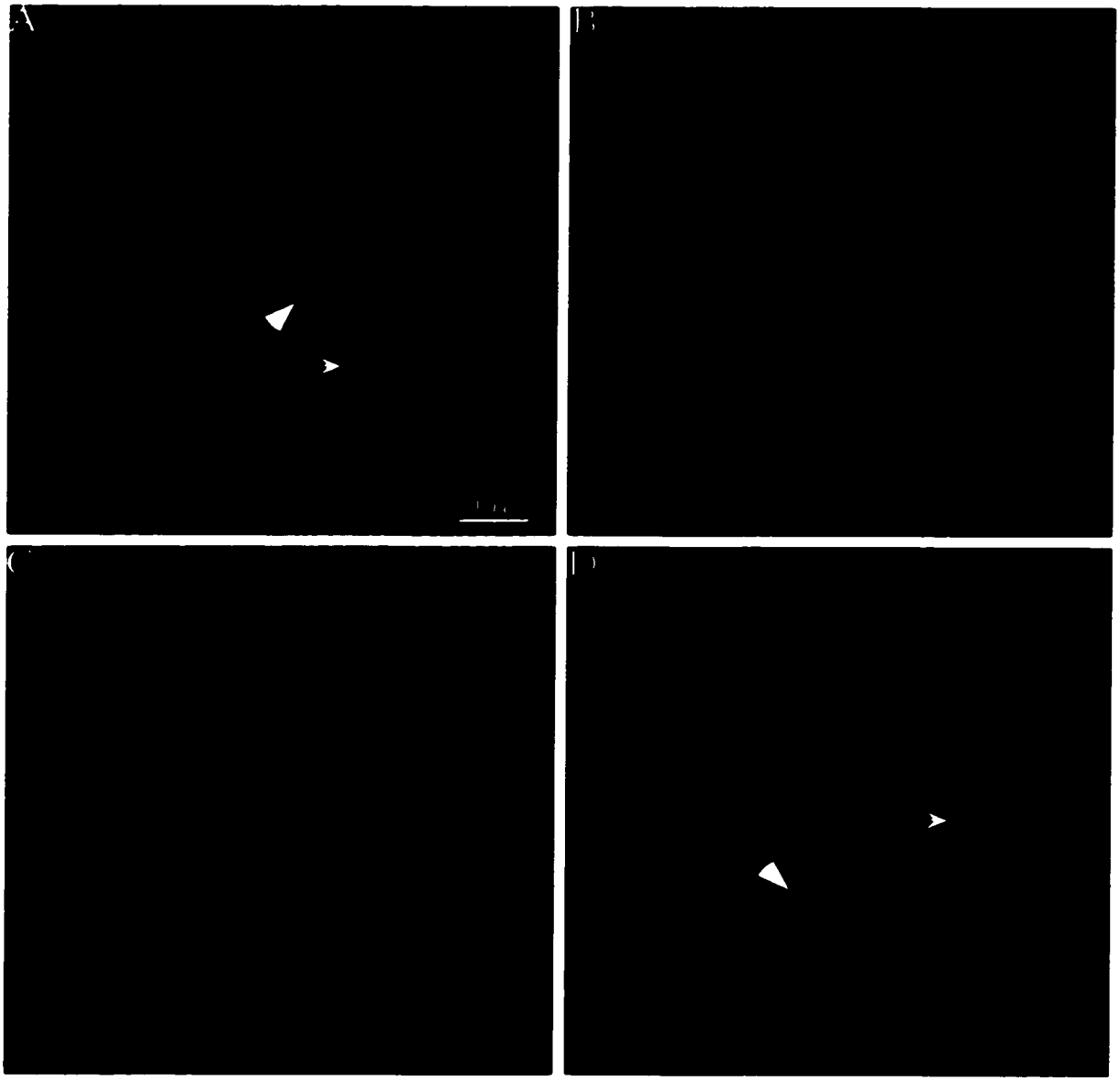

Figure 11. Schwann cell proliferation assay. **(A)** The FluorImager image of fluorescent densities in a 96 well plate from a single proliferation assay of cultures from 4 animals (2 wt, 1 het, 1 ko) from a single litter. Even numbered rows show the dilution series (0, 500, 1000, 2000, 5000 and 10,000 cells) used to convert pixel volumes to cell numbers for each culture. (Culture #129 did not have a well of 10,000 cells.) Odd numbered rows show triplicate wells from each culture that were untreated (basal), or treated with 75 ng/ml GGF or 10 mM TEA. **(B)** A graph demonstrating cell proliferation of the cultures shown in A. The pixel volumes from the triplicate wells of each culture condition were converted to cell numbers and averaged . Error bars represent standard error.

A.

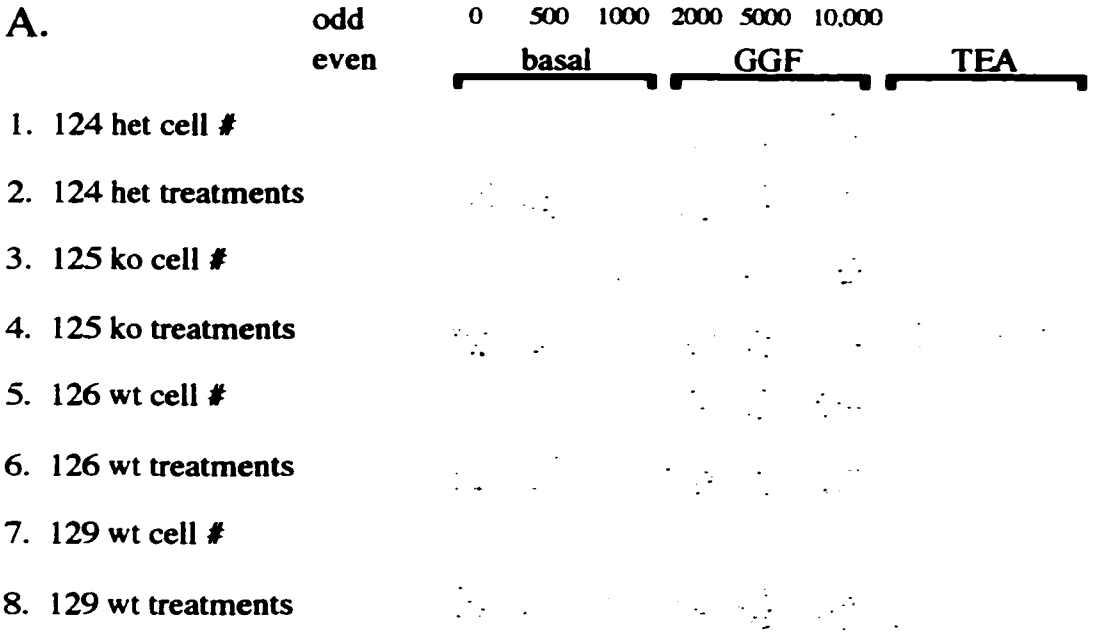
odd
even
0
500
1000
2000
5000
10,000
basal
GGF
TEA
1. 124 het cell #
2. 124 het treatments
3. 125 ko cell #
4. 125 ko treatments
5. 126 wt cell #
6. 126 wt treatments
7. 129 wt cell #
8. 129 wt treatments

B.

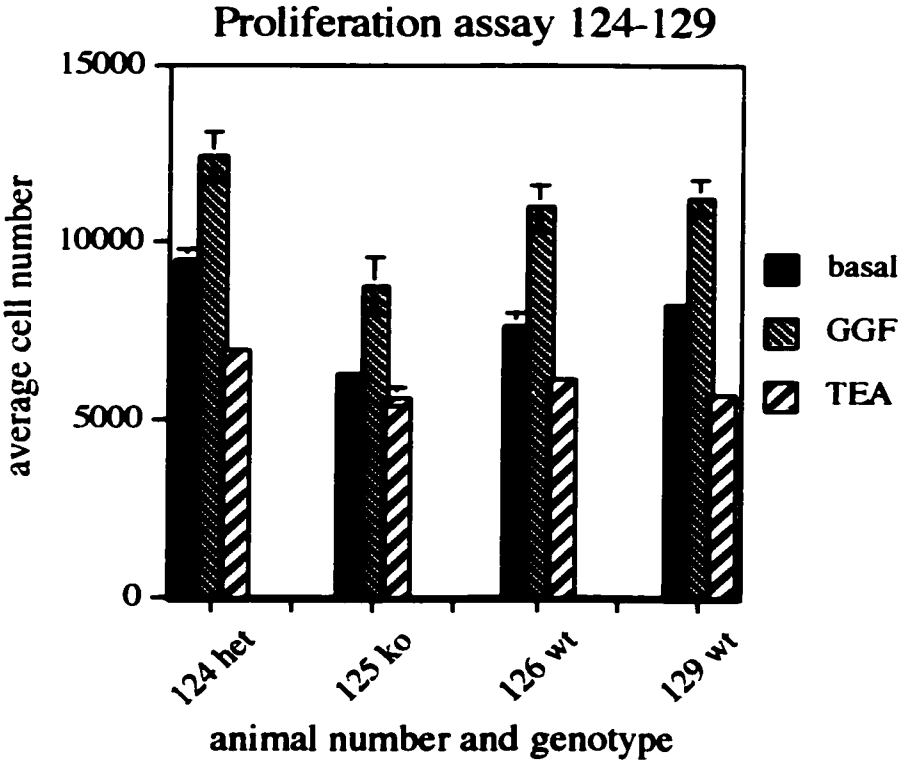
Proliferation assay 124-129
15000
10000
5000
0
average cell number
basal
GGF
TEA
124 het
125 ko
126 wt
129 wt
animal number and genotype

Figure 12. Combined proliferation data from all cultures. The means of triplicate wells from each individual animal of a given genotype (8 wt, 9 het, 8 ko) were averaged together for each culture condition. **(A)** Bar graph and **(B)** line graph of average cell numbers separated by genotype. These graphs demonstrate decreased proliferation in ko cultures compared to either wt or het cultures. **(C)** Bar graph of average cell numbers separated by treatment or culture condition. This graph demonstrates a consistent trend of decreased proliferation of ko cultures under all 3 culture conditions. Error bars represent standard error.

A.

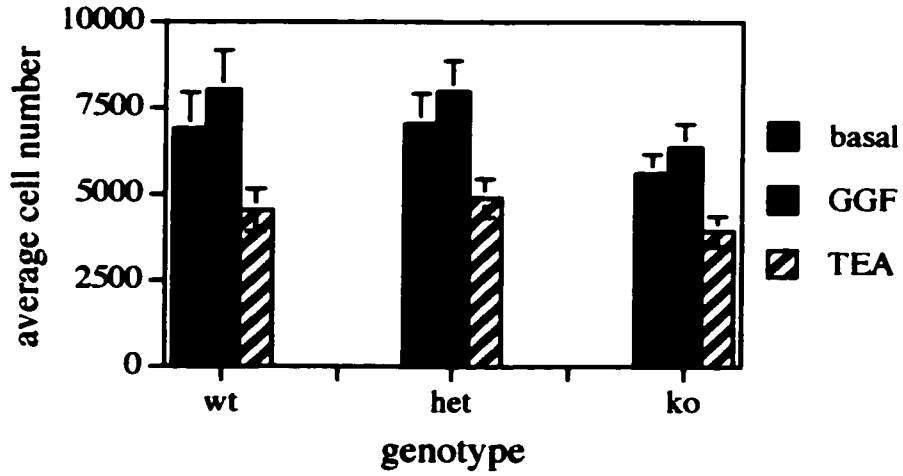
10000
7500
5000
2500
0
average cell number
wt
het
ko
genotype
basal
GGF
TEA

B.

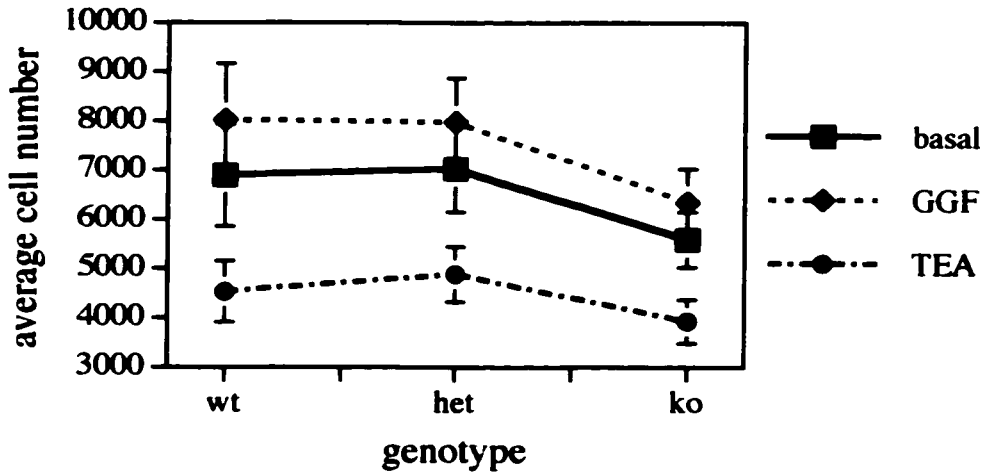
10000
9000
8000
7000
6000
5000
4000
3000
average cell number
wt
het
ko
genotype
basal
GGF
TEA

C.

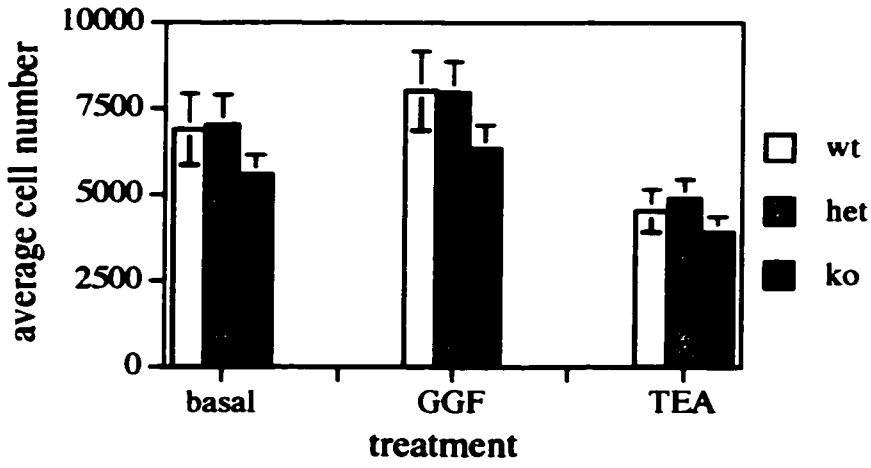
10000
7500
5000
2500
0
average cell number
basal
GGF
TEA
treatment
wt
het
ko

CHAPTER 5: REDISTRIBUTION OF Kv CHANNEL SUBUNITS DURING POSTNATAL DEVELOPMENT AND DISRUPTION IN *quivering* MICE.

Introduction

Saltatory transmission along axons is dependent on a variety of specialized microdomains or compartments within or adjacent to axons, including insulating myelin internodes, nodes of Ranvier, and regions of high ion channel densities at or near the nodes (see fig. 13a and b). In mature myelinated axons, high densities of voltage-gated Na^+ (Na) channels are found in the nodal gap, where they are responsible for the upstroke of the action potential (reviewed in (Hille, 1992). Mature mammalian peripheral nerves also contain clusters of voltage-gated K^+ (Kv) channels in juxtaparanodal zones, or regions adjacent to paranodes but under the myelin (Wang, Kunkel et al., 1993) (fig. 13a and b). The significance of Kv channel localization under the myelin is unclear, but recent evidence indicates these channels are involved in regulating neuronal excitability (Smart, Lopantsev et al., 1998; Vabnick, Trimmer et al., 1999).

Development of myelin and ion channel densities occurs postnatally. Peripheral nerves of newborn rats are virtually devoid of myelin, do not contain detectable ion channel clusters, and do not exhibit saltatory conduction. Shortly after birth, Schwann cell processes begin to surround single axons (Jacobson, 1991). Around the same time, Na channels begin a process of redistribution from a diffuse axonal localization towards nodes of Ranvier (Dugandzija-Novakovic, Koszowski et al., 1995; Vabnick, Novakovic et al., 1996). Finally, Kv channels begin to cluster in juxtaparanodal zones (Vabnick, Trimmer et al., 1999). The redistribution of both Na and Kv channels in the rat PNS is a very dynamic process that involves formation of transient, intermediate cluster types; however, the signals responsible for this redistribution remain unidentified.

We previously noted in mouse that Kv1.1 is evenly distributed along the lengths of embryonic PNS axons (chapter 2), while others found that Kv channels are clustered in the juxtaparanodal regions in the adult periphery (Wang, Kunkel et al., 1993). We have examined the dynamic redistribution of Kv (and Na) channels in sciatic nerve during

murine postnatal development, and report a similar sequence of channel clustering and the formation of transient cluster types as recently reported in rats.

To begin to understand the signals responsible for ion channel clustering, we have examined the localization of Kv and Na channels in the CNS and sciatic nerve of the neurological mouse mutant *quivering* (*qv*). *Quivering* first arose as a spontaneous mutation in 1953 at Ohio State University (Yoon, 1957). The mutation responsible for *qv* was identified as autosomal recessive, and homozygous *qv* mice are characterized by locomotor instability, pronounced quivering with increasing age, varying degrees of hindlimb paralysis, infertility in males, deafness, and shortened lifespan (Yoon, 1957). The cause of deafness in *qv* mice is thought to be central in origin (Bock, Frank et al., 1983). Six additional alleles of *qv* have been identified: qv^{J}, qv^{2J}, qv^{3J}, qv^{4J}, qv^{5J}, and qv^{6J} (MGD, 1999). The gene responsible for the *qv* phenotype has been mapped to mouse chromosome 7 (Yoon, 1957; Bronson, Sweet et al., 1992) but is as yet unidentified. We examined ion channel localization in the sciatic nerve in the original *qv* allele, in an allele with an intermediate hindlimb phenotype (qv^{4J}), and in a severely affected allele that was first identified in a screen for lumbosacral neuroaxonal dystrophy (qv^{6J}). Additionally, we examined ion channel localization in the CNS of qv^{6J} mice. We report disruption in localization of both Kv and Na channels in the sciatic nerves of all three *quivering* alleles; Kv1.1 channels fail to achieve mature juxtaparanodal localization and Na channels appear less concentrated in the nodes of Ranvier. Kv channel localization is also disrupted in the CNS of qv^{6J} mice. Additionally, nerve conduction velocities are reduced in the three *quivering* alleles to varying degrees. Both the degree of channel mislocalization and decrease in nerve conduction velocity correlates with the severity of the hindlimb phenotype. Finally, we report that peripheral myelin is delaminated in the most severely affected allele, qv^{6J}. Hence, a mutation in a single locus disrupts most if not all the microdomains necessary for saltatory conduction in the periphery.

Materials and methods

Animals

C3HeB/FeJ (C3H), C57BL/6By-qv^{4J} (qv^{4J}) and C3H/HeJ-qv^{6J} (qv^{6J}) mice from Jackson Labs and CBA/Gr-*qv* (*qv*) mice from Karen Steele in Nottingham, England were maintained in our colony and breeding pairs or trios established. The day of birth was designated postnatal day 0 (P0), the following day P1, and so forth. Mice were maintained on a 12 hour light/dark cycle according to approved animal care protocols, with food and water available *ad lib*. C3H mice were chosen as our wildtype (wt) strain to allow rigorous comparison to the qv^{6J} mice.

Immunocytochemistry

Sciatic nerves were removed at P0, at 3 day intervals from P3-P24, and at 4 weeks from wt mice, and at 4 weeks from qv and qv^{4J} and qv^{6J} mice. Nerves were fixed for 3 hours on ice in 4% paraformaldehyde (PFA), washed in PBS, cryoprotected in sucrose, frozen in OCT, cut in10 μm longitudinal sections on a cryostat, and mounted on chrome-alum slides. Alternatively, some 4 week old mice were intracardially perfused with 4% paraformaldehyde in PBS prior to nerve dissection (similar results were obtained with either method). Brains were also removed from 4 week old perfused animals, processed in the same manner as nerves, and cut in 20 μm sagittal sections on a cryostat. ICC was performed as in chapter 2 with the following primary antibodies: polyclonal anti-Kv1.1 at 1:50 (Wang, Kunkel et al., 1993); polyclonal anti-Kv1.2 at 1:200 (Rhodes, Keilbaugh et al., 1995) (gift of J. Trimmer, State University of New York at Stronnybrook, Long Island); polyclonal anti-Na at 1:200 (Dugandzija-Novakovic, Koszowski et al., 1995) (gift of R. Levinson, University of Colorado, Denver); monoclonal anti-S-100 at 1:1000 (Sigma). Fluorescent secondary antibodies (1:500) were goat anti-rabbit/Alexa 488 or 594 for polyclonal antibodies and goat anti-mouse/Alexa 488 or 594 for monoclonal antibodies (Molecular Probes). Images were collected on an MRC 1024 scanning confocal microscope (BioRad), processed in Adobe Photoshop, labeled in Deneba Canvas, and printed on a Tektronix SD II dye sublimation printer or an Epson Stylus 3000 color inkjet printer.

Transmission electronmicroscopy

4 week old wt and qv^{6J} mice were deeply anesthetized with CO_2, intracardially perfused with 4% paraformaldehyde, then sciatic nerves dissected and fixed in 3% gluteraldehyde/2% PFA in phosphate buffer at 4 °C for 16-18 hours. Nerves were washed in PBS, fixed in 1% OsO_4 on ice for 1 hour, washed again in PBS, dehydrated in ethanol, then transitioned to and mounted in plastic resin (Ted Pella, Inc.). Semi-thin cross sections were cut at 1 μm and stained with 1% toluidine blue; ultrathin sections were cut at 90nm, contrasted with uranyl acetate and lead citrate, and examined using a Jeol 1200EX transmission electron microscope. Images were captured on type 4489 film, and standard black and white prints made.

Electrophysiology

24-28 day old wt (n=6), *qv* (n=5), qv^{4J} (n=6) and qv^{6J} (n=6) mice were anesthetized with intraperitoneal injections of ketamine (0.08 mg/g) and xylazine (0.008 mg/g) and anesthesia maintained with 1/3 dose of each drug as needed. The entire length of the left sciatic nerve and its posterior tibial branch were exposed, and the segments near the spinal cord and the hind paw completely isolated from all surrounding tissue under a dissecting microscope. The animal was stretched out face down and attached to a peg board, and the lower half of its body immersed in a box containing mineral oil. The temperature of the mineral oil was maintained at 37 °C by a thermostatically controlled heat lamp (in a few experiments, the temperature varied between 36.5 and 38 °C). Hook electrodes were fashioned from 0.01 inch diameter paired silver wires that were insulated with teflon except for the hook portion. The distance between the paired wires within the hook portion was maintained at 1mm. The stimulating electrode was positioned under the proximal portion of the sciatic nerve near the spinal cord, and the recording electrode at the distal end of the tibial nerve near the paw (see fig. 19). Care was taken to insure electrodes made good contact with the nerve and did not touch surrounding tissue. The length of the nerve was measured between the distal end of the stimulating electrode and

the proximal end of the recording electrode by means of a compass. It should be noted that nerve length, and thus calculated conduction velocities, are probably underestimated because the entire length of the nerve was not completely dissected from surrounding tissue and our measurements could not account for all the contours of the tissue.

Electrical stimulation of the nerves was provided by a Grass SD9 stimulator (square wave with a duration of 0.04 msec at a rate of 2 per second). The recording electrode was connected to a Grass P55 AC preamplifier (100x, 0.3-3kHz filter). The evoked compound action potentials were displayed on a Tektronix RM200 oscilloscope and recorded via a Neuro Data Neuro-corder DR-390 to videotape for off-line analysis. Stimulation was begun at 0.1 volts and increased in 0.02 volt increments until the peak-to-peak amplitude of the compound action potential showed no further increase (maximal response). The minimum intensity of stimulus required to evoke a visibly detectable action potential was defined as the threshold stimulus. The time between the stimulus artifact at the intensity required to evoke a maximal response and the first deflection of the compound action potential was defined as the onset latency. Conduction velocity was calculated by dividing the nerve length between electrodes by the onset latency.

Results

Developmental redistribution of ion channels in mouse sciatic nerve

We performed ICC with antibodies specific to ion channels (Na, Kv1.1, and Kv1.2) to determine if the dynamic redistribution of Na and Kv channels in mouse sciatic nerves during postnatal development was similar to that recently reported in rat. An antibody to the myelin protein S-100 was also used to identify paranodes and nodes of Ranvier.

Both types of ion channels were diffusely localized along the length of axons and no myelin was detected at birth (fig. 14a and e). At P3, Na channels were found both in clusters at presumptive nodes and distributed along the length of axons; clusters were broad and usually composed of pairs (fig. 14b). By P9, myelin sheaths were discernable and Na channels were often found in single or paired broad clusters at presumptive nodes

(fig. 14c). By P12, some broad paired clusters of Na channels were still detected, but most clusters were narrow dense bands at nodes similar to clusters detected in mature mice (fig. 14d).

Redistribution of Kv channels began later in development than was detected for Na channels; both Kv1.1 and Kv1.2 subunits undergo the same pattern of postnatal redistribution, but for convenience, only the results for Kv1.1 are shown and discussed. The first clusters of Kv channels were detected at P6, and were either single (data not shown) or paired broad clusters (fig. 14f). Most Kv immunostaining at P6 was still distributed along the length of axons. By P9, most of the Kv channel clusters were pairs of clusters adjacent to both ends of nodes, and many pairs had a banded appearance, with one band at the paranode and one band adjacent to the paranode under the forming myelin sheath (juxtaparanodal) (fig. 14g and h). At P18, some Kv channel clusters were still paired banded clusters, while others where paired (not banded) juxtaparanodal clusters similar to the localization found in mature mice (fig. 14i and j). Little Kv channel immunostaining was distributed along the length of axons by P18.

Disruption of ions channel localization in sciatic nerves of quivering *mice*

To determine if Na and Kv channel localization is altered in *quivering* mice, we performed ICC on sciatic nerves of 4 week old wt, *qv*, qv^{4J}, and qv^{6J} mice using antibodies to Na channels, Kv1.1, and the myelin protein S-100. Myelin staining is shown only where it does not interfere with visualization of channel staining. In wt mice, Na channels were tightly clustered in nodes of Ranvier (fig. 15a), and Kv channels were clustered in juxtaparanodal regions (fig. 16a). The myelin in wt mice had a smooth rounded appearance at paranodes (fig. 15a) . In *qv* mice, both Na and Kv channels were still predominantly clustered in their normal domains, but Na channels appeared less dense in the nodes (fig. 15b) and Kv channel clusters had a banded appearance typical of immature axons (fig. 16b). Myelin in *qv* mice had an irregular bulky characteristic (fig. 15b). A similar pattern of ion channel disruption was detected in qv^{4J} mice but was slightly more apparent than in *qv* mice, and myelin appeared similar to that in *qv* mice

(fig. 15c, 16c). In qv^{6J} sciatic nerves, nodes of Ranvier became difficult to detect by either myelination or ion channel clustering (fig. 15d, 16d). Na channels were dispersed along the length of axons and clusters in nodes only rarely detected. Kv channel clusters were heavily banded, and the band nearest the node was sometimes appeared to be within the node instead of under the paranode.

Disruption of Kv channel localization in the CNS of quivering *mice*

To determine if ion channel localization in the CNS was different in wt and qv^{6J} mice, we performed ICC with antibodies to Na channels, Kv1.1 and S-100 on sagittal brainstem sections. Because qv^{6J} mice are deaf, we focused on ion channel localization in two regions of the auditory system: the entry point of the 8th nerve into the brainstem and in the trapezoid body.

In wt brainstem sections, Kv channel immunostaining was detected in a punctate pattern indicative of juxtaparanodal localization in axons of the 8th nerve and fiber tracts of the trapezoid body (fig. 17a and c). Kv1.1 signal was robust in cell bodies of the medial nucleus of the trapezoid body (MNTB), and was detected in a punctate pattern in axons emerging from these cells (fig. 17c). In qv^{6J} sections, Kv1.1 signal was no longer punctate in axons of the 8th nerve, trapezoid body fiber tracts, or axons emerging from MNTB somata, but was distributed along the length of axons (fig. 17b and d).

Na channel immunostaining was widespread in the entire brainstem in a punctate pattern. No obvious difference in Na channel localization was detected between wt and qv^{6J} mice in either the 8th nerve or the trapezoid body (fig. 17e and f).

Disruption of myelin in qv^{6J} *sciatic nerves*

Because the myelin in all 3 alleles of *quivering* appeared abnormal in ICC experiments, we examined the myelin in cross sections of sciatic nerves from wt and qv^{6J} mice by transmission electronmicroscopy (TEM). Figure 18a shows a cross section through a wt sciatic nerve, with a single Schwann cell producing a normally compacted, thick myelin sheath surrounding a single axon. In qv^{6J} nerves, the relatively few layers of

myelin surrounding small caliber axons appeared normally compacted (fig. 18b). In large diameter axons in qv^{6J}, the innermost and outermost layers of myelin appeared normally compacted, but the middle layers were delaminated, with large irregular gaps between layers (fig. 18b). This data shows a specific disruption of only the middle layers of thick myelin sheaths.

Altered sciatic nerve function in quivering *mice*

We measured two physiological parameters, threshold stimulus and conduction velocity, to examine nerve function in *quivering* sciatic nerves compared to wildtype. Figure 19 shows a drawing representing the surgeries and electrode placements for these experiments. The results of these experiments are presented in table 3.

Each animal was given a subjective hindlimb dysfunction rating from 0 to 5 prior to anesthesia (table 3). All wildtype animals were considered to have normal hindlimb function and were assigned ratings of 0. A dysfunction rating of 1 indicated a relatively normal gait with mild quivering. A rating of 2 indicated that the animal walked relatively normally but with some hesitation, and the quivering was more pronounced. A rating of 3 indicated the animal's gait was visibly affected by the degree of quivering. An animal that walked only with difficulty and often fell on its side was given a rating of 4. Complete hindlimb paralysis was given a rating of 5. As seen in table 1, the dysfunction ratings correlated with the severity of the allele; *qv* mice ranged from 1-2, qv^{4J} mice from 2-3, and qv^{6J} mice from 2.5-4. It should be noted that two qv^{6J} mice received dysfunction ratings of 5, but were excluded from the analysis; in one case the recording temperature was approximately 34 °C and the other the animal did not survive long enough to obtain recordings.

Most nerves had simple biphasic compound action potentials, with (fig. 20c) or without (fig. 20a,d and e) a small deflection in the initial portion of the action potential. Occasionally, wave forms were more complex (fig. 20b). The more complex wave forms were most often seen in wt (2 of 6) and *qv* (3 of 5) nerves, but were also seen in one qv^{4J}

and one qv^{6J} nerve and hence were not considered relevant to strain-specific nerve function.

A scattergram showing threshold stimuli from each individual animal by strain and the average threshold stimuli for each strain are presented in figure 21 and table 3, respectively. The threshold stimuli for most wt (5 of 6) and *qv* (5 of 5) nerves were below 0.3 volts, while thresholds for most qv^{4J} (4 of 6) and qv^{6J} (3 of 5) nerves were above 0.3 volts. A one-way analysis of variance confirmed that the means differed significantly between strains ($F[3, 19]=3.51$, $p=0.035$). Post hoc tests (Fisher's least squared difference) revealed a significant difference between wt and qv^{6J} ($p=0.04$), but not between wt and qv^{4J} ($p=0.08$). Both qv^{4J} and qv^{6J} threshold stimulus values were significantly different from *qv* values ($p=0.028$ and 0.015 respectively). A single wt sciatic nerve had a threshold stimulus value approximately 2-fold higher than the average (table 1, figure 8a); if this single value is excluded from the analysis, wt threshold stimulus values become significantly different from qv^{4J} values ($p=0.01$). These data suggest that qv^{4J} and qv^{6J} sciatic nerves may be less readily excited than wt or *qv* nerves.

Conduction velocity data is presented in figure 22 and table 3. The distribution of velocities by strain shows no overlap in values between wt animals and those of any *quivering* allele (fig. 22a). Among the *quivering* animals there is only a small degree of overlap between *qv* and qv^{4J} or qv^{6J} values. The averages of conduction velocities by strain show that wt nerves had the fastest conduction velocities (mean 20.47 m/sec), followed by *qv* nerves (mean 15.62 m/sec), then qv^{4J} nerves (mean 13.13 m/sec), and qv^{6J} velocities were the slowest (mean 12.8 m/sec) (fig. 22b, table 3). A one-way analysis of variance showed a significant effect of strain on conduction velocity ($F[3,18]=23.41$, $p<0.001$), and post-hoc statistical tests (Fisher's least squared difference) revealed a statistical difference between all strains except between qv^{4J} and qv^{6J}. These data demonstrate that all 3 alleles of *quivering* have slow sciatic nerve conduction velocities compared to wt, and that the degree of slowing correlates to a large extent with the severity of the hindlimb phenotype, our dysfunction ratings, and changes in nerve stimulus threshold levels.

Discussion

We have shown that the developmental redistributions of both Na and Kv channels in mouse sciatic nerve are similar to the patterns reported in rats, with Na channel clustering occurring earlier in postnatal development than that of Kv channels. In rat, early (P1-P3) Na channel clusters have been described as broad bands or pairs of bands at presumptive nodes, while more mature clusters are single dense, narrow bands (Dugandzija-Novakovic, Koszowski et al., 1995; Vabnick, Novakovic et al., 1996). We have detected similar types of Na channel clusters in mouse between P3 and P9. In 6-8 day old rat sciatic nerves or remyelinating nerves, early Kv channel clusters are detected, and are sometimes found within the nodal gap (Rasband, Trimmer et al., 1998; Vabnick, Trimmer et al., 1999). We first detected Kv channel clusters in mouse sciatic nerves at about the same age (P6), but found that the earliest clusters were paranodal and were not detected within the nodal gap. In rat sciatic nerves, intermediate (P14-P21) Kv channel clusters consisted of banded pairs of clusters adjacent to either end of a node, with one band in the paranode and a second band further under the myelin (Vabnick, Trimmer et al., 1999). We observed the formation of similar transient, banded clusters in developing mouse sciatic nerve starting at a somewhat earlier developmental age (P9-P18). Hence there are both similarities and minor differences in the dynamic redistribution of ion channels in postnatal rat and mouse sciatic nerves. These findings suggest that similar signals are responsible for ion channel clustering in both rat and mouse.

Our studies also demonstrate that both Na and Kv channel localization and nerve function are disrupted in 3 alleles of *quivering* mice. It is interesting to note that the degree of ion channel mislocalization and slowing of conduction velocity correlates to the severity of the hindlimb phenotype reported in these mice. This finding reflects the intimate structure-function relationship in myelinated axons. In the case of Kv channels, all 3 mutant *quivering* alleles exhibited a banded pattern of localization at 4 weeks that was similar to that found in immature sciatic nerves (P9-P18), suggesting that the mutated gene is required for at least the late stages of Kv channel clustering. In contrast,

Na channel clusters in all 3 mutant alleles appeared to be less dense versions of the narrow bands found in nodes of mature sciatic nerves; broad paired clusters were never detected. These findings suggest that the gene mutated in *quivering* mice is necessary for the maintenance of Na channel clusters. Because the gene mutated in *quivering* mice remains unknown, mutants can only be identified phenotypically at this time. The phenotype becomes apparent around 2 weeks of age, at which time ion channel clustering is well underway. Hence, definitive studies of the gene's role in the formation or maintenance of ion channel clusters await molecular identification of the gene, which will enable genotyping of animals prior to the onset of channel clustering.

Peripheral myelin also appeared abnormal in all 3 *quivering* alleles in ICC experiments, and was clearly disrupted in qv^{6J} sciatic nerves when examined by TEM. We have recently examined myelin in the CNS of qv^{6J} mice by TEM (data not shown), and found delamination of myelin present in the CNS as well. . This is in contrast to a previous report that the CNS of *qv* mice exhibited no morphological abnormalities in myelin (McNutt, 1962); however, the light microscopic technique used by McNutt detects only the presence or absence of myelin and we have not detected any regions completely lacking myelin in qv^{6J} mice. We also found that the disruption of peripheral myelin in qv^{6J} mice was a specific anomaly resulting in disruption of only the middle layers of thick myelin surrounding large caliber axons. It is unclear if the affected large diameter axons represent axons from a specific subpopulation of neurons, or if the defect is present in any axon which acquires a thick myelin sheath.

We have also demonstrated that Kv channels, but not necessarily Na channels, are mislocalized in the auditory brainstem of qv^{6J} mice. This finding is interesting in relation to what is known about the cause of deafness in *qv* mice. The cochleas are normal in these mice and hair cells do not degenerate with age. Cochlear action potential thresholds, amplitudes and latencies are normal; however, inferior colliculus evoked responses have longer latencies, elevated thresholds and decreased amplitudes (Bock, Frank et al., 1983). Cochlear nucleus evoked responses are also abnormal in *qv* mice; the second peak evoked in response to a tone is smaller in amplitude and has longer latencies

than normal controls (Bock and Frank, 1984). Given the proposed functions of Kv1.1 in regulating neuronal excitability and our findings that Kv channels are mislocalized in at least two structures of the auditory pathway (8th nerve and trapezoid body), our data suggests that Kv channel mislocalization in the CNS may contribute the hearing defect in *quivering* mice.

What type of protein might be mutated in *quivering* mice that produces both the specific myelin defect and ion channel mislocalization we detected? One possibility is that the mutation is in a cell adhesion molecule that is required for the formation and/or maintenance of compact myelin, and that normally compacted myelin is needed for mature ion channel localization. This hypothesis is consistent with the findings of others that Kv channels fail to attain their mature localization in two hypomyelinating mouse mutants, *shiverer* and *trembler* (Wang, Allen et al., 1995). Additionally, structures resembling intermediate paired Na channel clusters have been detected in sciatic nerves of adult *trembler* mice (Lambert, Davis et al., 1997). It is interesting to note that in the CNS of *shiverer* mice, there is an upregulation of a specific subtype of Na channels (Westenbroek, Noebels et al., 1992). We did not detect any obvious changes in Na channel localization in the CNS of qv^{6J} mice, but our experiments were not designed to detect subtype-specific upregulation.

Finally, our data shows that the mutation responsible for the *quivering* phenotype disrupts the axonal microanatomy necessary for saltatory conduction in peripheral nerves. The slow conduction velocity and disruption of myelin in the periphery suggests that *quivering* may be a mouse model for the human condition Charcot-Marie-Tooth Type 1. In humans, this condition is characterized by slow nerve conduction velocity with muscle weakness and atrophy in the extremities. Additionally, humans with CMS have varying degrees of hearing deficits. All of the genes responsible for this disorder that have been identified to date affect myelination, and includes the same mutation found in *trembler* mice (Chance, 1999).

Table 3. Nerve function data from wildtype and *quivering* mice

strain	Animal #	age	dysfunc-tion rating	threshold stimulus	onset latency	nerve length	conduction velocity
wt	4	24 days	0	0.18 volts	0.54 msec	13.5 mm	25.0 m/sec
wt	12	24	0	0.28	1.06	19.75	18.63
wt	13	24	0	0.16	0.93	19.5	20.97
wt	16	25	0	0.22	1.09	20.5	18.81
wt	17	25	0	0.22	1.11	21	18.92
wt	21	28	0	0.4	0.96	18.2	18.96
qv	1	25	1	0.22	0.98	14	14.29
qv	11	24	1	0.18	1	16	16
qv	18	26	1	0.2	1	16	16
qv	23	28	2	0.26	1.19	19	15.97
qv	24	28	1	0.22	1.2	19	15.83
qv ^{4J}	5	26	3	0.26	1.24	16	12.9
qv ^{4J}	8	25	2	0.36	1.32	17	12.88
qv ^{4J}	9	25	2	0.44	1.19	14	11.76
qv ^{4J}	14	26	3	0.32	1.11	14	12.61
qv ^{4J}	15	26	2	0.22	1.16	19	16.38
qv ^{4J}	22	27	2.5	0.32	1.51	18.5	12.25
qv ^{6J}	3	28	2.5	0.28	0.84	10	11.9
qv ^{6J}	6	25	3	0.42	0.85	12	14.12
qv ^{6J}	7	25	2.5	0.3	1	14	14
qv ^{6J}	10	25	4	0.44	1.22	14	11.48
qv ^{6J}	19	27	4	0.28	1.3	16	12.31
qv ^{6J}	20	25	4	0.28	1.23	16	13.01

Figure 13. Axonal microdomains required for saltatory conduction. **(A)** A diagram of a neuron depicting the microanatomy of myelinated axons. Insulating segments of myelin (internodes) wrap the axon. The spaces between the internodes (nodes of Ranvier) are filled with Na channels. Paranodes are formed where the upper layers of myelin stretch over lower layers and terminate in endfeet at the axonal membrane. Dense clusters of Kv channels are located next to the paranodes under the myelin sheath (juxtaparanodal zones). **(B)** Fluorescent ICC of a 4 week old C3H sectioned sciatic nerve stained with antibodies to Kv1.1 (green) and the myelin protein S-100 (red) depicting axonal microanatomy. Thin red lines define the myelin internodes. Paranodes are formed where the myelin crosses over the axon at the ends of internodes. Nodes of Ranvier are the spaces between the internodes (arrows). Dense clusters of Kv1.1 are found in juxtaparanodal regions (arrowheads). The soma of a Schwann cell is seen in the middle of the image (asterisk). Na channel clusters are not stained.

Figure 14. Developmental redistribution of Na (A-D) and Kv (E-J) channels in mouse sciatic nerves by fluorescent ICC. **(A)** A P0 sciatic nerve stained for Na channels detected distribution of channels along the length of axons. Myelin sheaths were not detected. **(B)** At P3, Na channel staining was still robust along the lengths of axons, and broad paired clusters of Na_v channels were often detected (arrows). The paired nature of the clusters is not readily seen in the printed images and is apparent only by the contours or notches seen at the edges of clusters. **(C)** In P9 sciatic nerves, Na channels are less readily detected along the lengths of axons, and single and paired (arrow) broad clusters are detected. Myelin sheaths were readily detected (arrowhead). **(D)** At P12, Na channel clusters are either broad (arrowhead) or dense narrow bands (arrows). **(E)** A P0 nerve stained with antibodies to Kv1.1 detected distribution of the channel along the length of axons. Myelin sheaths were not detected. **(F)** At P6, Kv1.1 most channels were still distributed along the length of axons but some paired channel clusters were detected (arrowheads). **(G)** At P9, some axons still had Kv1.1 channel subunits distributed along their length, but pairs of clusters were readily detected (arrowheads). Myelin sheaths were readily detected (arrows). **(H)** A higher magnification of a P9 nerve stained with anti-Kv1.1 demonstrating the banded nature of many of the pairs of Kv channel clusters. The outer bands were in juxtaparanodal regions (arrowheads) and the smaller inner bands were much closer to or within the paranode (arrows). **(I)** At P18, most Kv channels were clustered in the juxtaparanodal regions (arrowheads), and inner bands were often seen in the paranodes (arrows). **(J)** A higher magnification of a P18 sciatic nerve stained with anti-Kv1.1 demonstrating the banded nature of some channel clusters, with large dense clusters in the juxtaparanodal regions (arrowheads) and smaller clusters in the paranodes (arrows).

Figure 15. Localization and Na channels (green) and myelin internodes (myelin protein S-100 in red) in 4 week old wt and *quivering* sectioned sciatic nerves. **(A)** In wt (C3H) mice, myelin was smooth and rounded at paranodes, and Na channels formed dense clusters in the nodes of Ranvier (arrows). **(B)** In *qv* nerves, myelin had an irregular, bulky appearance and Na channels appeared less densely packed (arrows). **(C)** In qv^{4J} nerves, myelin had a similar appearance as in *qv* mice, and Na channel density at nodes appeared even less dense (arrows). **(D)** In qv^{6J} nerves, myelin was similar to *qv* and qv^{4J} nerves in appearance, and Na channel densities in nodes were difficult to detect (arrows). Na channels were readily detected distributed along the lengths of axons (arrowheads).

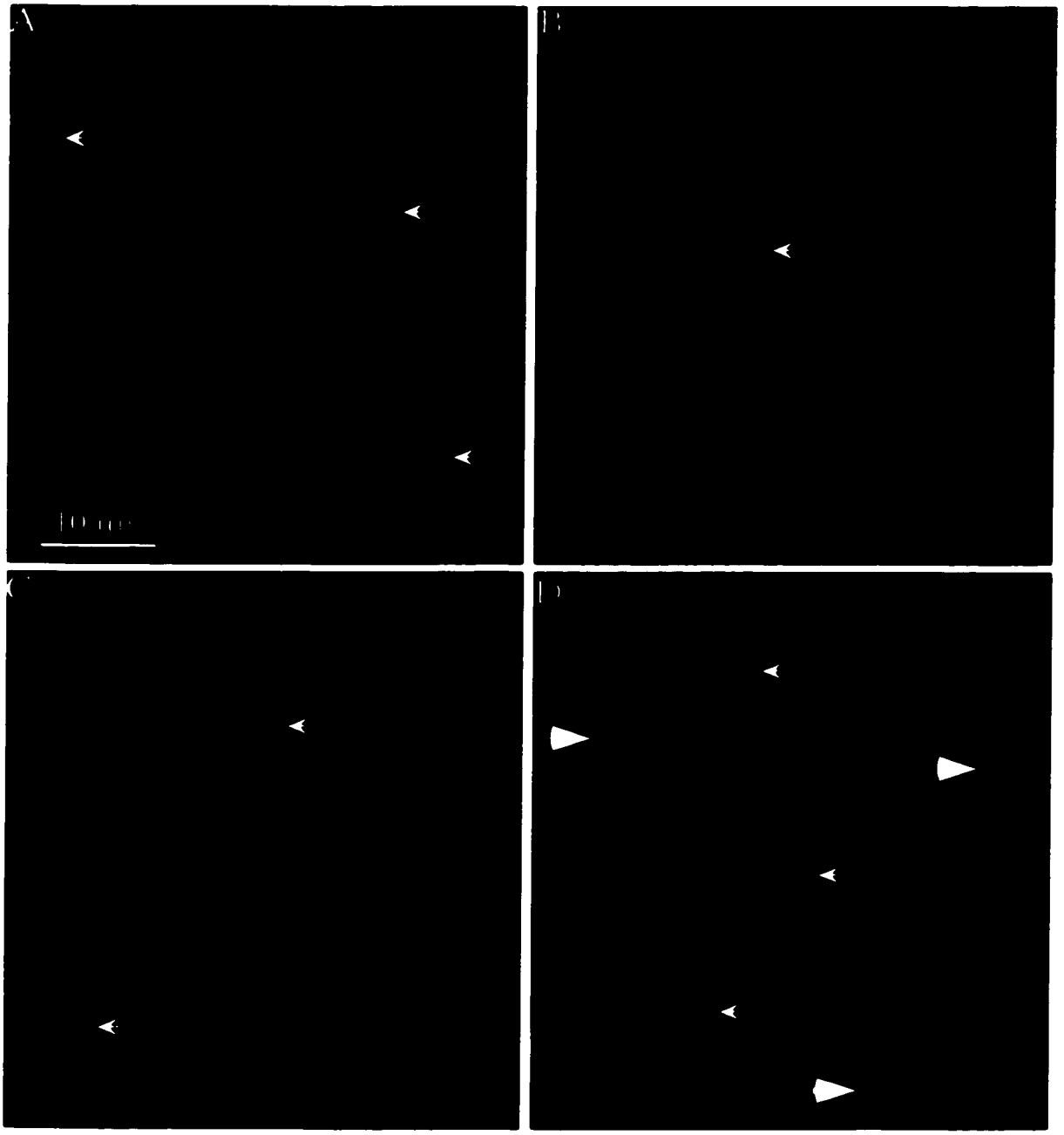
A
B
C
D

Figure 16. Localization of Kv1.1protein in 4 week old wt and *quivering* sciatic nerves. **(A)** In wt (C3H) nerves, most Kv1.1 immunostaining was clustered in juxtaparanodal regions (arrowheads). **(B)** In *qv* nerves, clustering of Kv1.1 in juxtaparanodes was dense in large diameter axons (arrowheads), but paranodal clustering was also detected (arrows). **(C)** In qv^{4J} nerves, Kv1.1 was occasionally concentrated in juxtaparanodal regions (arrowheads), but most axons had distinct banded clusters in the paranodal regions. **(D)** In qv^{6J} nerves, Kv1.1 staining was found in juxtaparanodal regions (arrowheads), paranodes and nodes (arrows).

A
B
C
D

Figure 17. Localization of Kv1.1 and Na_v channel proteins in the auditory brainstem of 4 week old wt and qv^{6J} mice. Coronal brainstem sections were stained with antibodies to Kv1.1 (green) and S-100 (red) in A-D, and antibodies to Na channels (green) and S-100 (red) were used in panels E and F. **(A)** The 8th (auditory) nerve of a wt C3H mouse at its point of entry into the brainstem had a very punctate pattern of Kv1.1 staining, indicative of juxtaparanodal localization. **(B)** In the 8th nerve of a qv^{6J} mouse, Kv1.1 staining was strongly detected along the length of axons. **(C)** In the trapezoid body of a wt C3H mouse, Kv1.1 signal was robust in the somata of primary neurons in the medial nucleus (MNTB; arrowhead), and immunostaining of trapezoid body fiber tracts (arrows) and axons from MNTB neurons was very punctate. **(D)** In the trapezoid body of a qv^{6J} mouse, Kv1.1 staining was robust in the somata of MNTB neurons and also distributed along the axons emerging from these neurons (arrowhead). In the fiber tracts of the trapezoid body, Kv1.1 staining was distributed along the length of axons (arrow). **(E)** Na channel signal was very punctate in both the fiber tracts of the trapezoid body (arrows) and in the MNTB. **(F)** Na channel staining in the trapezoid body of a qv^{6J} mouse was not appreciably different from that of the wt pattern, and was detected in a punctate pattern in trapezoid body fiber tracts (arrows) and in the MNTB.

Figure 18. Sciatic nerve morphology in 4 week old wt and *qv6J* mice by TEM. The nuclei of individual Schwann cells are marked N. **(A)** Cross section of a wt C3H nerve shows normally compacted myelin surrounding both small (open arrow) and large diameter (filled arrow) axons. **(B)** Cross section of a qv^{6J} nerve demonstrating normally compacted myelin around small diameter axons (open arrows), but delaminated middle layers of myelin around large diameter axons (filled arrows). Scale bar represents 1 μm.

Figure 19. Sciatic nerve surgery and electrode placement. The sciatic nerve and its posterior tibial branch were exposed along its entire length in the left leg of each animal. The nerve was completely dissected free of all surrounding tissue near the spinal cord for placement of the stimulating electrode, and near the paw for placement of the recording electrode.

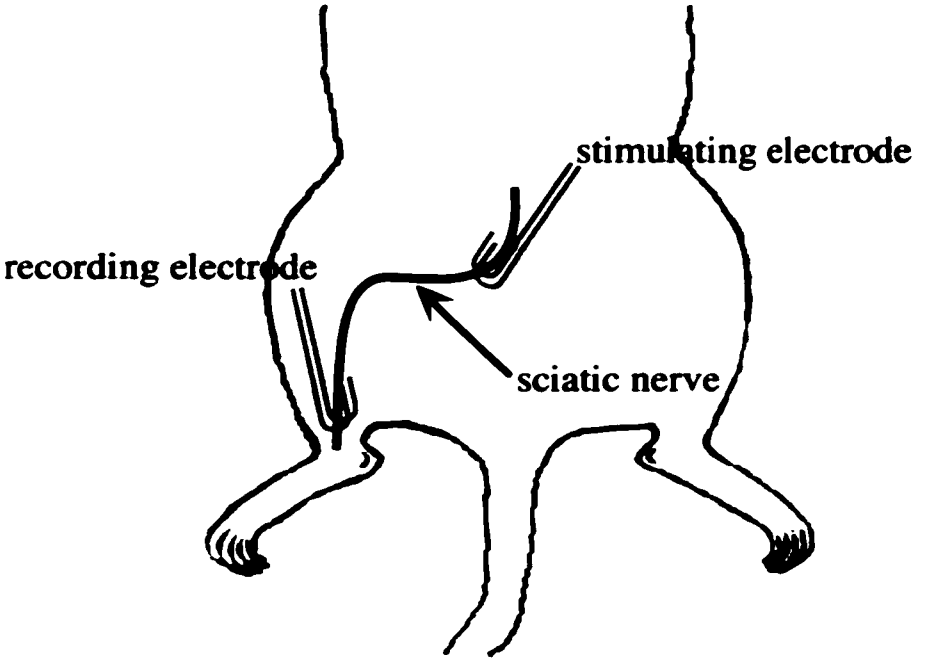
stimulating electrode
recording electrode
sciatic nerve

Figure 20. Evoked compound action potentials from sciatic nerves of 4 week old wt **(A, B)**, *qv* **(C)**, qv^{4J} **(D)**, and qv^{6J} **(E)** mice demonstrating the various waveforms obtained. The onset latency for each nerve was as the time between the stimulation artifact (arrowheads) and the first deflection of the action potential from baseline (arrows). Note that in C, there was a small initial downward deflection from baseline that is not apparent at this scale. Sale bars represent 1 mvolt, 1 msec.

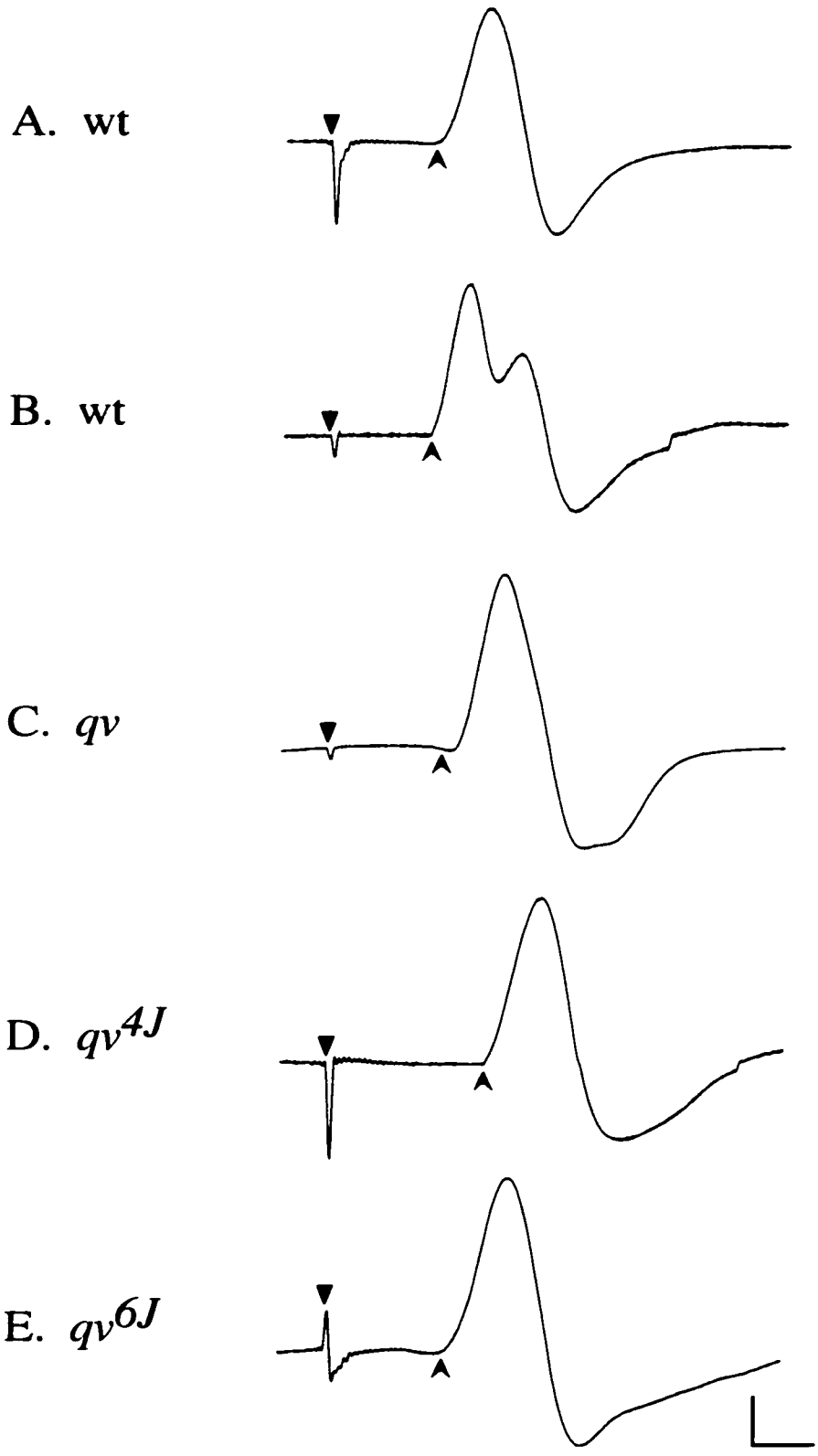
A. wt
B. wt
C. qv
D. qv4J
E. qv6J

Figure 21. Threshold stimulus data for evoked action potentials. **(A)** A scattergram showing the threshold stimulus values for all animals used in this study separated by strain (wt and qv^{4J} n=6, qv and qv^{6J} n=5). **(B)** The average values for threshold stimuli by strain. Error bars represent standard error. * indicates $p < 0.05$.

A.

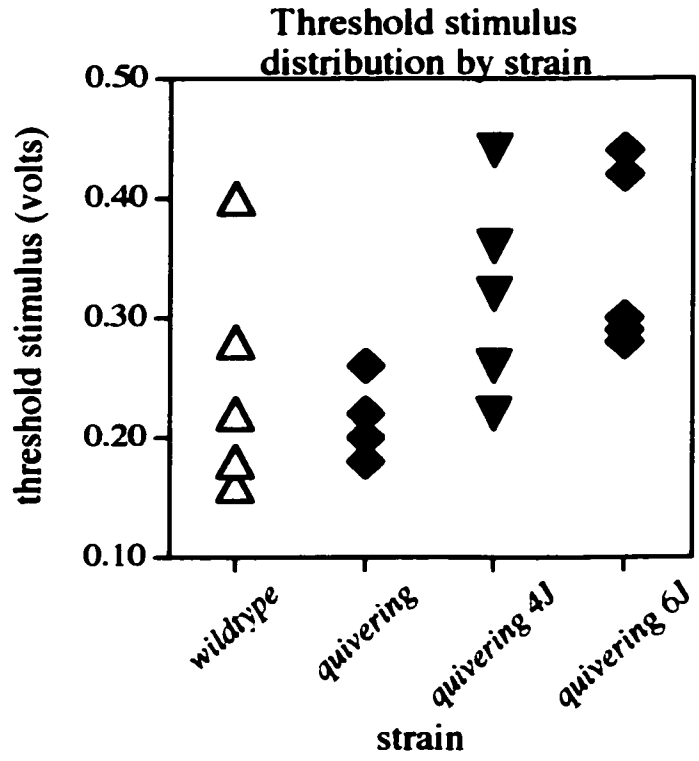
Threshold stimulus distribution by strain
threshold stimulus (volts)
0.50
0.40
0.30
0.20
0.10
wildtype
quivering
quivering 4J
quivering 6J
strain

B

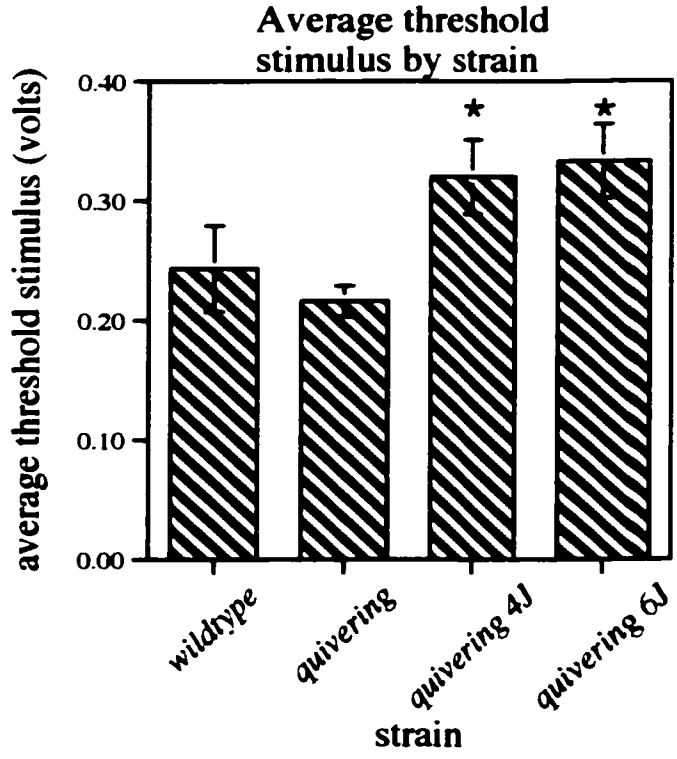
Average threshold stimulus by strain
average threshold stimulus (volts)
0.40
0.30
0.20
0.10
0.00
*
*
wildtype
quivering
quivering 4J
quivering 6J
strain

Figure 22. Conduction velocity data for evoked action potentials. **(A)** A scattergram showing the conduction velocity values for all animals used in this study separated by strain wt, qv^{4J} and qv^{6J} n=6, *qv* n=5). **(B)** The average values for conduction velocities by strain. Error bars represent standard error. * indicates $p < 0.05$; ** indicates $p < 0.001$.

A.

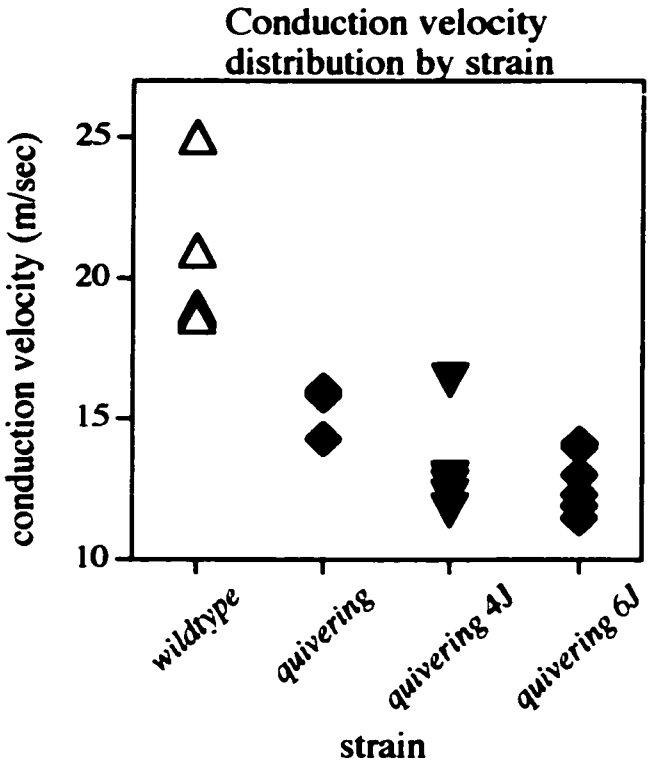
Conduction velocity distribution by strain
conduction velocity (m/sec)
25
20
15
10
wildtype
quivering
quivering 4J
quivering 6J
strain

B.

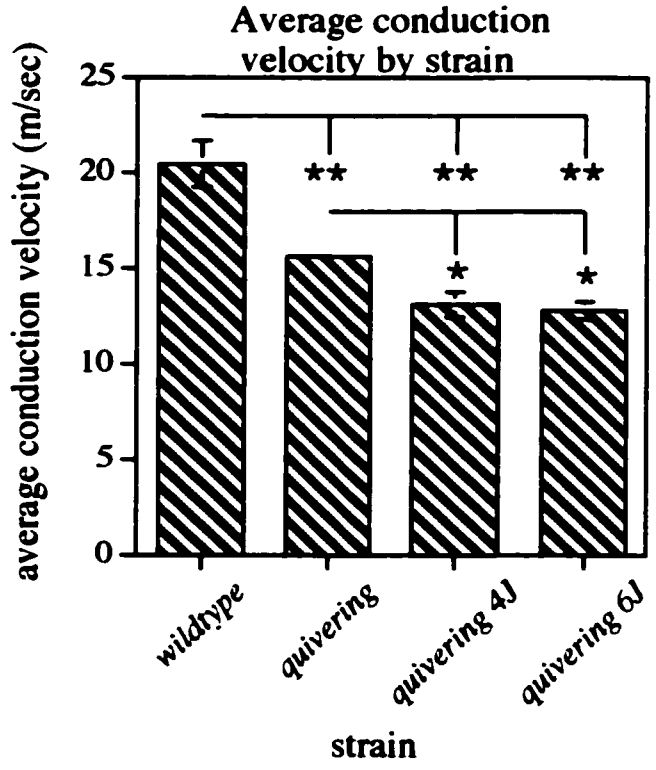
Average conduction velocity by strain
average conduction velocity (m/sec)
25
20
15
10
5
0
**
**
**
*
*
wildtype
quivering
quivering 4J
quivering 6J
strain

LIST OF REFERENCES

Aguilar-Bryan, L. and J. Bryan (1999). "Molecular biology of adenosine triphosphate-sensitive potassium channels." Endocr Rev **20**(2): 101-35.

Allen, M. L., D. S. Koh, et al. (1998). "Cyclic AMP regulates potassium channel expression in C6 glioma by destabilizing Kv1.1 mRNA." Proc Natl Acad Sci U S A **95**(13): 7693-8.

Alvarez-Buylla, A., D. R. Buskirk, et al. (1987). "Monoclonal antibody reveals radial glia in adult avian brain." Journal of Comparative Neurology **264**(2): 159-70.

Anton, E. S., M. Hadjiargyrou, et al. (1995). "CD9 plays a role in Schwann cell migration in vitro." J Neurosci **15**: 584-595.

Ausubel, F. M. (1992). Current Protocols in Molecular Biology. New York, Wiley & sons.

Barish, M. E. (1986). "Differentiation of voltage-gated potassium current and modulation of excitability in cultured amphibian spinal neurones." Journal of Physiology **375**: 229-50.

Barish, M. E. (1995). "Modulation of the electrical differentiation of neurons by interactions with glia and other non-neuronal cells." Perspect Dev Neurobiol **2**(4): 357-70.

Baumann, A., A. Grupe, et al. (1988). "Structure of the voltage-dependent potassium channel is highly conserved from Drosophila to vertebrate central nervous systems." Embo J **7**(8): 2457-63.

Beckh, S. and O. Pongs (1990). "Members of the RCK potassium channel family are differentially expressed in the rat nervous system." Embo J **9**(3): 777-82.

Bock, G. R. and M. P. Frank (1984). "Brainstem responses in the quivering mutant mouse." Acta Otolaryngol (Stockh) **98**(3-4): 193-8.

Bock, G. R., M. P. Frank, et al. (1983). "The quivering mutant mouse: hereditary deafness of central origin." Acta Otolaryngol (Stockh) **96**(5-6): 371-7.

Bosma, M. M., M. L. Allen, et al. (1993). "PKA-dependent regulation of mKv1.1, a mouse Shaker-like potassium channel gene, when stably expressed in CHO cells." Journal of Neuroscience **13**(12): 5242-50.

Bronson, R. T., H. O. Sweet, et al. (1992). "Genetic and age related models of neurodegeneration in mice: dystrophic axons." J Neurogenet **8**(2): 71-83.

Browne, D. L., S. T. Gancher, et al. (1994). "Episodic ataxia/myokymia syndrome is associated with point mutations in the human potassium channel gene, KCNA1 [see comments]." Nat Genet **8**(2): 136-40.

Burger, C. and A. B. Ribera (1996). "Xenopus spinal neurons express Kv2 potassium channel transcripts during embryonic development." Journal of Neuroscience **16**(4): 1412-21.

Carr, P. A. and J. I. Nagy (1993). "Emerging relationships between cytochemical properties and sensory modality transmission in primary sensory neurons." Brain Research Bulletin **30**(3-4): 209-19.

Chance, P. F. (1999). "Molecular genetics of hereditary neuropathies." J Child Neurol **14**(1): 43-52.

Chandy, K. G. and G. A. Gutman (1993). "Nomenclature for mammalian potassium channel genes." Trends Pharmacol Sci **14**(12): 434.

Chiu, S. Y. and G. F. Wilson (1989). "The role of potassium channels in Schwann cell proliferation in Wallerian degeneration of explant rabbit sciatic nerves." Journal of Physiology **408**: 199-222.

Chiu, S. Y., S. S. Scherer, et al. (1994). "Axons regulate the expression of Shaker-like potassium channel genes in Schwann cells in peripheral nerve." Glia **12**(1): 1-11.

Chomczynski, P. and N. Sacchi (1987). "Single-step method of RNA isolation by acid guanidinium thiocyanate-phenol-chloroform extraction." Analytical Biochemistry **162**(1): 156-9.

Cohan, C. S., J. A. Connor, et al. (1987). "Electrically and chemically mediated increases in intracellular calcium in neuronal growth cones." J Neurosci **7**(11): 3588-99.

Covarrubias, M., A. A. Wei, et al. (1991). "Shaker, Shal, Shab, and Shaw express independent K+ current systems." Neuron **7**(5): 763-73.

Damsky, C., A. Sutherland, et al. (1993). "Extracellular matrix 5: adhesive interactions in early mammalian embryogenesis, implantation, and placentation." Faseb J **7**(14): 1320-9.

deLatt, S. W. and J. G. Bluemink (1974). "New membrane formation during cytokinesis in normal and cytochalasin B-treated eggs of *Xenopus laevis*." J. Cell Biol. **60**: 529-540.

Desarmenien, M. G., B. Clendening, et al. (1993). "In vivo development of voltage-dependent ionic currents in embryonic Xenopus spinal neurons." Journal of Neuroscience **13**(6): 2575-81.

Dugandzija-Novakovic, S., A. G. Koszowski, et al. (1995). "Clustering of Na+ channels and node of Ranvier formation in remyelinating axons." J Neurosci **15**(1 Pt 2): 492-503.

Easter, S. S., Jr., L. S. Ross, et al. (1993). "Initial tract formation in the mouse brain." Journal of Neuroscience **13**(1): 285-99.

Emerit, M. B., M. Riad, et al. (1992). "Trophic effects of neurotransmitters during brain maturation." Biology of the Neonate **62**(4): 193-201.

Finkbeiner, S. and M. E. Greenberg (1996). "Ca(2+)-dependent routes to Ras: mechanisms for neuronal survival, differentiation, and plasticity?" Neuron **16**(2): 233-6.

Fraser, S., R. Keynes, et al. (1990). "Segmentation in the chick embryo hindbrain is defined by cell lineage restrictions." Nature **344**(6265): 431-5.

Goddard, J. M., M. Rossel, et al. (1996). "Mice with targeted disruption of Hoxb-1 fail to form the motor nucleus of the VIIth nerve." Development **122**(10): 3217-28.

Goslin, K., D. J. Schreyer, et al. (1990). "Changes in the distribution of GAP-43 during the development of neuronal polarity." Journal of Neuroscience **10**(2): 588-602.

Grissmer, S., B. Dethlefs, et al. (1990). "Expression and chromosomal localization of a lymphocyte K+ channel gene." Proc Natl Acad Sci U S A **87**(23): 9411-5.

Grunwald, G. B. (1993). "The structural and functional analysis of cadherin calcium-dependent cell adhesion molecules." Curr Opin Cell Biol **5**(5): 797-805.

Gurantz, D., A. B. Ribera, et al. (1996). "Temporal regulation of Shaker- and Shab-like potassium channel gene expression in single embryonic spinal neurons during K+ current development." Journal of Neuroscience **16**(10): 3287-95.

Guthrie, S., V. Prince, et al. (1993). "Selective dispersal of avian rhombomere cells in orthotopic and heterotopic grafts." Development **118**(2): 527-38.

Hagiwara, S., S.-I. Miyasaki, et al. (1975). "Voltage clamp analysis of two inward current mechanisms in the egg cell membrane of a starfish." J. Gen. Physiol. **65**: 617-644.

Hatten, M. E., R. K. Liem, et al. (1986). "Weaver mouse cerebellar granule neurons fail to migrate on wild-type astroglial processes in vitro." Journal of Neuroscience **6**(9): 2676-83.

Heinemann, S. H., J. Rettig, et al. (1996). "Functional characterization of Kv channel beta-subunits from rat brain." J Physiol (Lond) **493**(Pt 3): 625-33.

Hille, B. (1992). Na and K channels of axons. Ionic Channels of Excitable Membranes. Sunderland, MA, Sinauer Associates Inc.: 59-81.

Hille, B. (1992). Potassium channels and chloride channels. Ionic Channels of Excitable Membranes. Sunderland, MA, Sinauer Associates, Inc.: 115-139.

Hopkins, W. F., M. L. Allen, et al. (1994). "Properties of voltage-gated K+ currents expressed in Xenopus oocytes by mKv1.1, mKv1.2 and their heteromultimers as revealed

by mutagenesis of the dendrotoxin-binding site in mKv1.1." Pflugers Arch **428**(3-4): 382-90.

Inoue, T., O. Chisaka, et al. (1997). "Cadherin-6 expression transiently delineates specific rhombomeres, other neural tube subdivisions, and neural crest subpopulations in mouse embryos." Dev Biol **183**(2): 183-94.

Isacoff, E. Y., Y. N. Jan, et al. (1990). "Evidence for the formation of heteromultimeric potassium channels in Xenopus oocytes [see comments]." Nature **345**(6275): P 530-4.

Jacobson, M. (1991). Developmental Neurobiology. New York, Plenum Press.

Jones, S. M. and A. B. Ribera (1994). "Overexpression of a potassium channel gene perturbs neural differentiation." Journal of Neuroscience **14**(5 Pt 1): 2789-99.

Kai, K.-M. A. (1989). "Cytochemistry of the trigeminal and dorsal root ganglia and spinal cord of the rat." Comparative Biochemistry and Physiology **93**(1): 183-93.

Komuro, H. and P. Rakic (1996). "Intracellular Ca2+ fluctuations modulate the rate of neuronal migration." Neuron **17**(2): 275-85.

Lambert, S., J. Q. Davis, et al. (1997). "Morphogenesis of the node of Ranvier: co-clusters of ankyrin and ankyrin-binding integral proteins define early developmental intermediates." J Neurosci **17**(18): 7025-36.

Letourneau, P. C., F. K. Roche, et al. (1991). "Interactions of Schwann cells with neurites and with other Schwann cells involve the calcium-dependent adhesion molecule, N-cadherin." J Neurobiol **22**(7): 707-20.

Letourneau, P. C., T. A. Shattuck, et al. (1990). "Nerve growth cone migration onto Schwann cells involves the calcium-dependent adhesion molecule, N-cadherin." Dev Biol **138**(2): 430-42.

Lewis, R. S. and M. D. Cahalan (1988). "Subset-specific expression of potassium channels in developing murine T lymphocytes." Science **239**(4841 Pt 1): 771-5.

Lockery, S. R. and N. C. Spitzer (1992). "Reconstruction of action potential development from whole-cell currents of differentiating spinal neurons." Journal of Neuroscience **12**(6): 2268-87.

Lumsden, A. and R. Keynes (1989). "Segmental patterns of neuronal development in the chick hindbrain." Nature **337**(6206): 424-8.

MacKinnon, R. (1991). "Determination of the subunit stoichiometry of a voltage-activated potassium channel." Nature **350**(6315): 232-5.

Maricich, S. M., J. Soha, et al. (1997). "Failed cell migration and death of purkinje cells and deep nuclear neurons in the weaver cerebellum." Journal of Neuroscience **17**(10): 3675-83.

Marrs, J. A. and W. J. Nelson (1996). "Cadherin cell adhesion molecules in differentiation and embryogenesis." Int Rev Cytol **165**: 159-205.

McNutt, W. (1962). "Urinary amino acid excretion in quivering mice (qv/qv)." Anat. Rec. **142**: 257.

M. G. D. (1999). Mouse Genome Informatics, The Jackson Laboratory, Bar Harbor, Maine. **1999**.

Mi, H., T. J. Deerinck, et al. (1995). "Differential distribution of closely related potassium channels in rat Schwann cells." Journal of Neuroscience **15**(5 Pt 2): 3761-74.

Misson, J. P., M. A. Edwards, et al. (1988). "Identification of radial glial cells within the developing murine central nervous system: studies based upon a new immunohistochemical marker." Brain Research **44**(1): 95-108.

Moody, S. A., M. S. Quigg, et al. (1989). "Development of the peripheral trigeminal system in the chick revealed by an isotype-specific anti-beta-tubulin monoclonal antibody." Journal of Comparative Neurology **279**(4): 567-80.

Moody, W. J. (1985). "The development of calcium and potassium currents during oogenesis in the starfish, Leptasterias hexactis." Developmental Biology **112**(2): 405-13.

Moody, W. J., L. Simoncini, et al. (1991). "Development of ion channels in early embryos." Journal of Neurobiology **22**(7): 674-84.

Naciff, J. M., M. M. Behbehani, et al. (1996). "Annexin VI modulates Ca2+ and K+ conductances of spinal cord and dorsal root ganglion neurons." American Journal of Physiology **271**(6 Pt 1): C2004-15.

Nagafuchi, A., S. Tsukita, et al. (1993). "Transmembrane control of cadherin-mediated cell-cell adhesion." Semin Cell Biol **4**(3): 175-81.

Nakahira, K., G. Shi, et al. (1996). "Selective interaction of voltage-gated K+ channel beta-subunits with alpha-subunits." J Biol Chem **271**(12): 7084-9.

Neely, M. D. and M. Gesemann (1994). "Disruption of microfilaments in growth cones following depolarization and calcium influx." J Neurosci **14**(12): 7511-20.

Nieto, M. A., L. C. Bradley, et al. (1992). "Molecular mechanisms of pattern formation in the vertebrate hindbrain." Ciba Foundation Symposium **165**: 92-102; discussion 102-7.

O'Dowd, D. K., A. B. Ribera, et al. (1988). "Development of voltage-dependent calcium, sodium, and potassium currents in Xenopus spinal neurons." Journal of Neuroscience **8**(3): 792-805.

Ohya, S., M. Tanaka, et al. (1997). "Molecular cloning and tissue distribution of an alternatively spliced variant of an A-type K+ channel alpha-subunit, Kv4.3 in the rat." FEBS Lett **420**(1): 47-53.

Papazian, D. M., T. L. Schwarz, et al. (1987). "Cloning of genomic and complementary DNA from Shaker, a putative potassium channel gene from Drosophila." Science **237**(4816): 749-53.

Papazian, D. M., L. C. Timpe, et al. (1991). "Alteration of voltage-dependence of Shaker potassium channel by mutations in the S4 sequence." Nature **349**(6307): 305-10.

Patil, N., D. R. Cox, et al. (1995). "A potassium channel mutation in weaver mice implicates membrane excitability in granule cell differentiation." Nature Genetics **11**(2): 126-9.

Perney, T. M., J. Marshall, et al. (1992). "Expression of the mRNAs for the Kv3.1 potassium channel gene in the adult and developing rat brain." J Neurophysiol **68**(3): 756-66.

Rader, R. K., L. E. Kahn, et al. (1996). "T cell activation is regulated by voltage-dependent and calcium- activated potassium channels." J Immunol **156**(4): 1425-30.

Rakic, P. and H. Komuro (1995). "The role of receptor/channel activity in neuronal cell migration." J Neurobiol **26**(3): 299-315.

Rasband, M. N., J. S. Trimmer, et al. (1998). "Potassium channel distribution, clustering, and function in remyelinating rat axons." J-Neurosci **18**(1): P 36-47.

Rettig, J., S. H. Heinemann, et al. (1994). "Inactivation properties of voltage-gated K+ channels altered by presence of beta-subunit." Nature **369**(6478): 289-94.

Rhodes, K. J., S. A. Keilbaugh, et al. (1995). "Association and colocalization of K+ channel alpha- and beta-subunit polypeptides in rat brain." J Neurosci **15**(7 Pt 2): 5360-71.

Rhodes, K. J., M. M. Monaghan, et al. (1996). "Voltage-gated K+ channel beta subunits: expression and distribution of Kv beta 1 and Kv beta 2 in adult rat brain." J Neurosci **16**(16): 4846-60.

Ribera, A. B. (1996). "Homogeneous development of electrical excitability via heterogeneous ion channel expression." Journal of Neuroscience **16**(3): 1123-30.

Ribera, A. B. and D. A. Nguyen (1993). "Primary sensory neurons express a Shaker-like potassium channel gene." Journal of Neuroscience **13**(11): 4988-96.

Ribera, A. B. and N. C. Spitzer (1989). "A critical period of transcription required for differentiation of the action potential of spinal neurons." Neuron **2**(1): 1055-62.

Ribera, A. B. and N. C. Spitzer (1991). "Differentiation of delayed rectifier potassium current in embryonic amphibian myocytes." Developmental Biology **144**(1): 119-28.

Rizzo, M. A. and W. Nonner (1992). "Transient K current in the somatic membrane of cultured central neurons of embryonic rat." Journal of Neurophysiology **68**(5): 1708-19.

Roy, M. L., D. Saal, et al. (1996). "Manipulation of the delayed rectifier Kv1.5 potassium channel in glial cells by antisense oligodeoxynucleotides." Glia **18**(3): 177-84.

Ruppersberg, J. P., K. H. Schroter, et al. (1990). "Heteromultimeric channels formed by rat brain potassium-channel proteins [see comments]." Nature **345**(6275): 535-7.

Scott, V. E., Z. M. Muniz, et al. (1994). "Antibodies specific for distinct Kv subunits unveil a heterooligomeric basis for subtypes of alpha-dendrotoxin-sensitive K+ channels in bovine brain." Biochemistry **33**(7): 1617-23.

Simoncini, L., M. L. Block, et al. (1988). "Lineage-specific development of calcium currents during embryogenesis." Science **242**(4885): 1572-5.

Smart, S. L., M. M. Bosma, et al. (1997). "Identification of the delayed rectifier potassium channel, Kv1.6, in cultured astrocytes." Glia **20**(2): 127-34.

Smart, S. L., V. Lopantsev, et al. (1998). "Deletion of the Kv1.1 Potassium Channel Causes Epilepsy in Mice." Neuron **20**: 1-20.

Sobko, A., A. Peretz, et al. (1998). "Heteromultimeric delayed-rectifier K+ channels in schwann cells: developmental expression and role in cell proliferation." J Neurosci **18**(24): 10398-408.

Soliven, B., S. Szuchet, et al. (1989). "Expression and modulation of K+ currents in oligodendrocytes: possible role in myelinogenesis." Dev Neurosci **11**(2): 118-31.

Sontheimer, H. (1994). "Voltage-dependent ion channels in glial cells." Glia **11**(2): 156-72.

Spruce, A. E. and W. J. Moody (1992). "Developmental sequence of expression of voltage-dependent currents in embryonic Xenopus laevis myocytes." Developmental Biology **154**(1): 11-22.

Stuhmer, W., M. Stocker, et al. (1988). "Potassium channels expressed from rat brain cDNA have delayed rectifier properties." FEBS Lett **242**(1): 199-206.

Surmeier, D. J., A. Stefani, et al. (1991). "Developmental regulation of a slowly-inactivating potassium conductance in rat neostriatal neurons." Neuroscience Letters **122**(1): 41-6.

Swanson, J. S., Marshall, J., Smith, J. S., Williams, J. B., Boyle, M. B., Folander, K., Luneau, C. J., Anatanavage, J., Olivia, C., Behrow, S. A., Bennet, C., Stein, R. B., Kaczmarek, L. K. (1990). "Cloning and expression of cDNA and genomic clones encoding three delayed-rectifier potassum channels in rat brain." Neuron **4**: 929-939.

Tempel, B. L., Y. N. Jan, et al. (1988). "Cloning of a probable potassium channel gene from mouse brain." Nature **332**(6167): 837-9.

Topilko, P., M.-S. Schneider, et al. (1994). "Krox-20 controls myelination in the peripheral nervous system." Nature **371**(6500): 796-9.

Tsaur, M. L., M. Sheng, et al. (1992). "Differential expression of K+ channel mRNAs in the rat brain and down- regulation in the hippocampus following seizures." Neuron **8**(6): 1055-67.

Vabnick, I., J. S. Trimmer, et al. (1999). "Dynamic potassium channel distributions during axonal development prevent aberrant firing patterns." J Neurosci **19**(2): 747-58.

Vabnick, I., S. D. Novakovic, et al. (1996). "The clustering of axonal sodium channels during development of the peripheral nervous system." J Neurosci **16**(16): 4914-22.

Veh, R. W., R. Lichtinghagen, et al. (1995). "Immunohistochemical localization of five members of the Kv1 channel subunits: contrasting subcellular locations and neuron-specific co- localizations in rat brain." Eur J Neurosci **7**(11): 2189-205.

Wang, H., M. L. Allen, et al. (1995). "Hypomyelination alters K+ channel expression in mouse mutants shiverer and Trembler." Neuron **15**(6): 1337-47.

Wang, H., D. D. Kunkel, et al. (1993). "Heteromultimeric K+ channels in terminal and juxtaparanodal regions of neurons." Nature **365**(6441): 75-9.

Wang, H., D. D. Kunkel, et al. (1994). "Localization of Kv1.1 and Kv1.2, two K channel proteins, to synaptic terminals, somata, and dendrites in the mouse brain." Journal of Neuroscience **14**(8): 4588-99.

Wang, S. Y., N. A. Castle, et al. (1992). "Identification of RBK1 potassium channels in C6 astrocytoma cells." Glia **5**(2): 146-53.

Westenbroek, R. E., J. L. Noebels, et al. (1992). "Elevated expression of type II Na+ channels in hypomyelinated axons of shiverer mouse brain." J Neurosci **12**(6): 2259-67.

Wilkinson, D. G., S. Bhatt, et al. (1989). "Segment-specific expression of a zinc-finger gene in the developing nervous system of the mouse." Nature **337**(6206): 461-4.

Williams, D. K. and C. S. Cohan (1995). "Calcium transients in growth cones and axons of cultured Helisoma neurons in response to conditioning factors." J Neurobiol **27**(1): 60-75.

Wilson, G. F. and S. Y. Chiu (1993). "Mitogenic factors regulate ion channels in Schwann cells cultured from newborn rat sciatic nerve." Journal of Physiology **470**: 501-20.

Wizenmann, A. and A. Lumsden (1997). "Segregation of rhombomeres by differential chemoaffinity." Molecular and Cellular Neurosciences **9**(5-6): 448-59.

Wu, R. L. and M. E. Barish (1994). "Astroglial modulation of transient potassium current development in cultured mouse hippocampal neurons." Journal of Neuroscience **14**(3 Pt 2): 1677-87.

Yellen, G., M. E. Jurman, et al. (1991). "Mutations affecting internal TEA blockade identify the probable pore- forming region of a K+ channel." Science **251**(4996): 939-42.

Yoon, C. H. and Les, E. P. (1957). "Quivering, a new first chromosome mutaion in mice." J. Hered. **48**: 176-180.

Zipes, D. P. a. J., J. (1995). Cardiac Electrophysiology, From Cell to Bedside, W.B. Saunders company.

Zona, C., F. Eusebi, et al. (1990). "Glycosylation is required for maintenance of functional voltage-activated channels in growing neocortical neurons of the rat." Proceedings of the Royal Society of London **239**(1295): 119-27.

Zuberi, S. M., L. H. Eunson, et al. (1999). "A novel mutation in the human voltage-gated potassium channel gene (Kv1.1) associates with episodic ataxia type 1 and sometimes with partial epilepsy." Brain **122**(Pt 5): 817-25.

CURRICULUM VITAE

Janice Lynn Hallows

Born January 25, 1956 - Aurora, IL

Position Graduate student, Department of Pharmacology, University of Washington, Seattle, WA

Address Department of Pharmacology, Box 357280
Health Sciences Building
University of Washington
Seattle, WA 98195

Education University of Missouri, Kansas City, MO; B. S. (1980)
University of Washington, Seattle, WA; (1993-1999)

Graduate School (1993-1999) Department of Pharmacology
University of Washington

Thesis Developmental Expression and Functions of Voltage-gated Potassium Channels in Normal and Mutant Mice

Advisor Bruce L Tempel, Ph.D.

Degree Ph.D. (1999)

Support Molecular Neurobiology Training Grant (1994-1995)
Pharmacological Sciences Training Grant (1995-1998)

Undergraduate (1976-1980) University of Missouri, Kansas City, MO
(1974-1975) University of Missouri, Columbia, MO

Degree (1980) B. S. with distinction

Honors (1978) Rho Chi national honorary pharmacy fraternity
(1980) Merck Award for excellence in pharmaceutical chemistry

Publications

Research Papers

1. Hallows, J. L. and Tempel, B. L (1998) Expression of Kv1.1, a Shaker-like potassium channel, is temporally regulated in embryonic neurons and glia. *J. Neurosci.* 18:5682-5691.

2. Hallows, J. L. and Tempel, B. L (1999) Differential expression of Shaker-like potassium channels during embryonic development. *In preparation.*

3. Hallows, J. L. and Tempel, B. L (1999) The role of Kv1.1 in Schwann cell proliferation. *In preparation.*

4. Hallows, J. L., Lippe, W., Cunningham, D., and Tempel, B. L (1999) Disruption of axonal microanatomy and sciatic nerve function in *quivering* mice. *In preparation.*

Abstracts

1. Brew, H. M., Hallows, J. L. and Tempel, B. L (1998) Hyperexcitability in auditory neurons of mice lacking the voltage-gated potassium channel gene, *Kcna* (Kv1.1). Molecular Biology of Hearing and Deafness Conference, Bethesda, MD.

2. Hallows, J. L. and Tempel, B. L (1998) Expression of Kv1.1, a Shaker-like potassium channel, is temporally regulated in embryonic neurons and glia. *Soc. Devel. Biol. Abstr.* as published in *Devel. Biol.* 198:196. Society for Developmental Biology Conference, Palo Alto, CA.

3. Fonseca, R. C., Hallows, J. L., Trimmer, J. S., Rhodes, K. J. and Tempel, B. L (1998) Localization of Kv channels in the auditory system. Association of Research in Otolaryngology Conference, St. Petersburg, FL.

4. Hallows, J. L. and Tempel, B. L (1996) Temporal expression and localization of a murine Shaker-like K^+ channel, mKv1.1, during embryonic development. Society for Neuroscience Conference, Washington, DC.